AD-A045 866 SOUTHWEST RESEARCH INST SAN ANTONIO TEX F/G 19/1
MAGNETIC PERTURBATION INSPECTION OF ARTILLERY PROJECTILES.(U)
SEP 77 R D WILLIAMS, J R BARTON DAAG46-76-C-0075
UNCLASSIFIED SWRI-15-4670 AMMRC-CTR-77-23 NL

| OF |
AD
A045866

END
DATE
FILMED
11-77
DDC

(12)

AMMRC CTR 77-23

MAGNETIC PERTURBATION INSPECTION OF ARTILLERY PROJECTILES

September 1977

Russell D. Williams
John R. Barton
Southwest Research Institute
P.O. Drawer 28510
San Antonio, Texas 78284

Final Report Contract Number DAAG46-76-C-0075

Prepared for

ARMY MATERIALS AND MECHANICS RESEARCH CENTER
Watertown, Massachusetts 02172

The findings in this report are not to be construed as an official Department of the Army position, unless so designated by other authorized documents.

Mention of any trade names or manufacturers in this report shall not be construed as advertising nor as an official indorsement or approval of such products or companies by the United States Government.

DISPOSITION INSTRUCTIONS

Destroy this report when it is no longer needed.
Do not return it to the originator.

SOUTHWEST RESEARCH INSTITUTE

8500 CULEBRA ROAD • POST OFFICE DRAWER 28510 • SAN ANTONIO, TEXAS 78284

25 October 1977

Subject: Final Technical Report
Contract DAAG46-76-C-0075, SwRI Project 15-4670
"Magnetic Perturbation Inspection of Artillery Projectiles"

Dear Sir:

Enclosed you will find a copy (o s) of the Final Report AMMRC CTR 77-23, entitled "Magnetic Perturbation Inspection of Artillery Projectiles," in accordance with the distribution list included at the end of the report.

Very truly yours,

John R. Barton

John R. Barton, Vice President
Instrumentation Research Division

RDW:jw
Encl.

UNCLASSIFIED

SECURITY CLASSIFICATION OF THIS PAGE (When Data Entered)

(19) REPORT DOCUMENTATION PAGE		READ INSTRUCTIONS BEFORE COMPLETING FORM
(18) 1. REPORT NUMBER: AMMRC CTR-77-23	2. GOVT ACCESSION NO.	3. RECIPIENT'S CATALOG NUMBER (9)
(6) 4. TITLE (and Subtitle): MAGNETIC PERTURBATION INSPECTION OF ARTILLERY PROJECTILES.		5. TYPE OF REPORT & PERIOD COVERED: Final Report. 8 Sept 76 – 7 Oct 1977
	(14)	6. PERFORMING ORG. REPORT NUMBER: SwRI-15-4670
(10) 7. AUTHOR(s): Russell D. Williams, John R. Barton	(15)	8. CONTRACT OR GRANT NUMBER(s): DAAG46-76-C-0075
9. PERFORMING ORGANIZATION NAME AND ADDRESS: Southwest Research Institute, 8500 Culebra Rd., P.O. Drawer 28510, San Antonio, Texas 78284		10. PROGRAM ELEMENT, PROJECT, TASK AREA & WORK UNIT NUMBERS: D/A Project: N/A; AMCMS Code: 4932.05.6654.0.02; Agency Accession:
11. CONTROLLING OFFICE NAME AND ADDRESS: Frankford Arsenal, Philadelphia, Pennsylvania 19137	(11)	12. REPORT DATE: Sept 1977
		13. NUMBER OF PAGES: 66
14. MONITORING AGENCY NAME & ADDRESS (if different from Controlling Office): Army Materials and Mechanics Research Center, Watertown, Massachusetts 02172 (12) 64 p.		15. SECURITY CLASS. (of this report): Unclassified
		15a. DECLASSIFICATION/DOWNGRADING SCHEDULE

16. DISTRIBUTION STATEMENT (of this Report)

Approved for public release; distribution unlimited.

DDC RECEIVED NOV 1 1977 F.

17. DISTRIBUTION STATEMENT (of the abstract entered in Block 20, if different from Report)

18. SUPPLEMENTARY NOTES

This project has been accomplished as part of the U.S. Army Manufacturing Methods and Technology Program, which has as its objective the timely establishment of manufacturing processes, techniques or equipment to insure the efficient production of current or future defense programs.

19. KEY WORDS (Continue on reverse side if necessary and identify by block number)

Nondestructive Testing
Projectiles
Cylindrical Shells
Magnetic Detection
Defects

20. ABSTRACT (Continue on reverse side if necessary and identify by block number)

The objectives of this research were to determine feasibility for the application of magnetic perturbation inspection methods to interior and exterior surfaces of artillery projectile casings. Inspections were performed on ten (10) projectiles. Subsequent metallurgical sectioning at seven (7) magnetically determined sites confirmed flaws at all selected locations. Feasibility of method was demonstrated. Basic conceptual design of a prototype inspection device is included.

DD FORM 1 JAN 73 1473 EDITION OF 1 NOV 65 IS OBSOLETE

UNCLASSIFIED

SECURITY CLASSIFICATION OF THIS PAGE (When Data Entered)

328 200

FOREWORD

This project was initiated under the Army Armament Command's program on Fragmentation Materials for Artillery Projectiles. Dr. S. K. Nash, Frankford Arsenal, was Project Manager and Mr. R. H. Brockelman, the AMMRC Contract Manager. Appreciation is expressed to Mr. Brockelman for his excellent guidance and cooperation throughout this program to demonstrate the feasibility for application of the magnetic perturbation method of inspection to the interior and exterior surfaces of the artillery projectile casings.

TABLE OF CONTENTS

LIST OF ILLUSTRATIONS

LIST OF ILLUSTRATIONS (Cont'd)

I. INTRODUCTION

The primary objective of this program was to develop a bench-type laboratory system to demonstrate the capability of the magnetic perturbation inspection method for detecting flaws in artillery projectiles. A photograph of a projectile is shown in Figure 1*. Complete inspection of the inside and outside surfaces and reliable detection of flaws oriented in either the circumferential or longitudinal directions with major dimensions of 0.050-in. long x 0.015-in. deep or larger is desired. Flaws of interest are: cracks, seams, cold shuts, splits and inclusions. Additionally, the bench-type system should demonstrate magnetizing techniques, scanning mechanisms and signal processing methods capable of performing inspections at a rate of several projectiles per minute.

Two existing laboratory systems were modified to accommodate the 155mm projectiles and to provide the scanning capability required for inspecting the areas of interest on the inside and outside surfaces. One of these systems, provided axial magnetization for maximum sensitivity to circumferentially oriented defects and the other provided circumferential magnetization which provides maximum sensitivity to axially oriented defects.

After completion of these equipment modifications, and the design and evaluation of promising probe configurations, inspections were performed on the ten (10) projectiles supplied; both axial and circumferential magnetization directions were utilized. These inspections covered in excess of 90% of the total projectile inside and outside surface areas. Time required for complete inspection of a projectile was approximately 2 minutes; by using inside and outside probes simultaneously the inspection could be accomplished in approximately 30 seconds.

An analysis of the inspection records was completed and metallurgical sectioning was performed at several selected sites. Results of these sectioning investigations disclosed either cracks or inclusions at all sectioning locations. Prominent examples of signatures and associated cracks are presented in Figure 2. Note that most of the signatures are observed for several revolutions, and since the probe is advanced 0.1-in./rev. the axial extent of the cracks can be determined easily. A more detailed analysis of these and other results will be presented later.

An overall analysis indicates that the magnetic perturbation method can provide a reliable, high speed, high sensitivity approach for an automated nondestructive examination to ensure material integrity of artillery projectiles. Subsequent sections of this report will present details on which the above forecast is based.

*These particular projectiles were selected because of their availability from a prior program in which they were part of a group inspected ultrasonically and rejected at the Iowa Army Ammunition Plant.

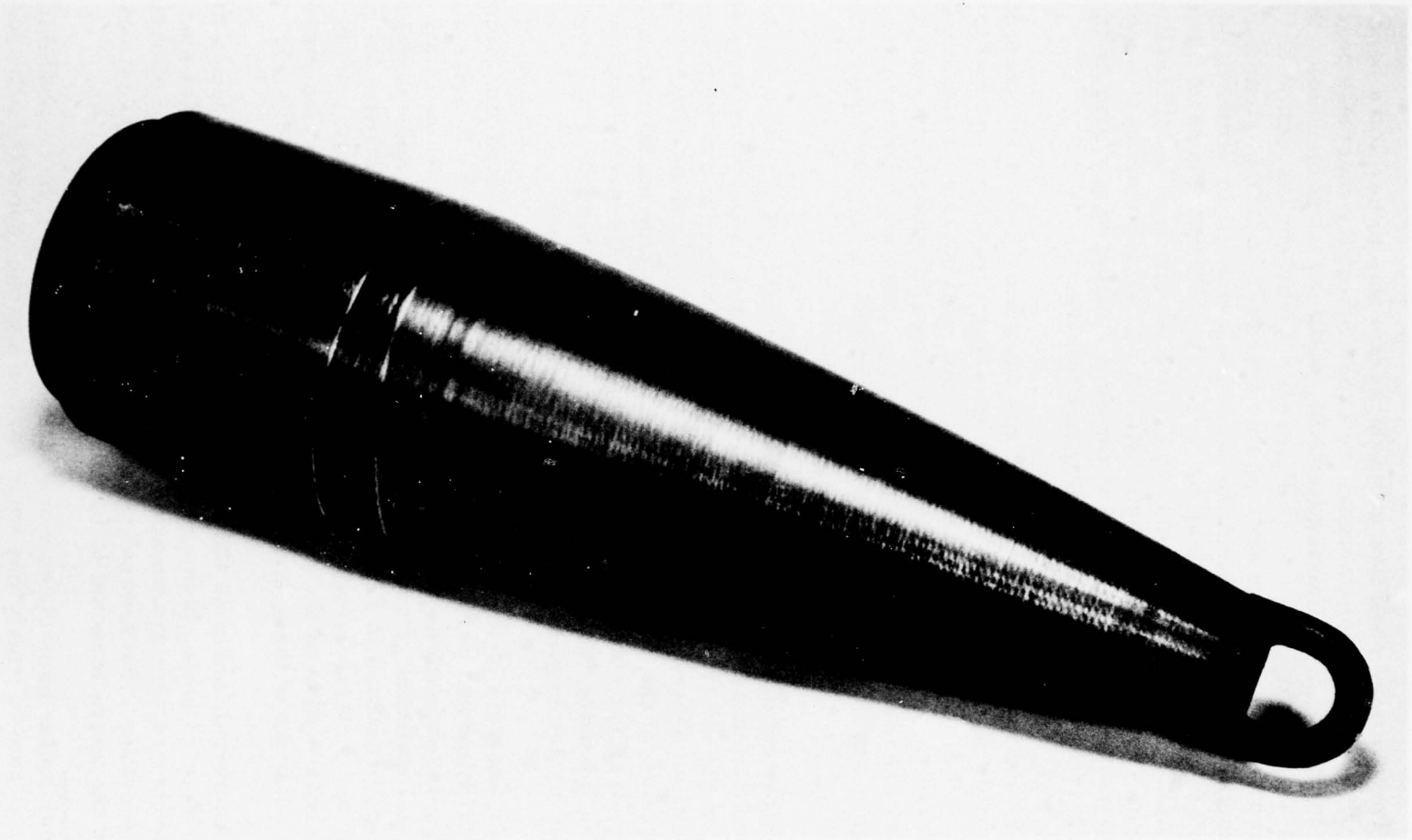

FIGURE 1. M549, 155MM PROJECTILE

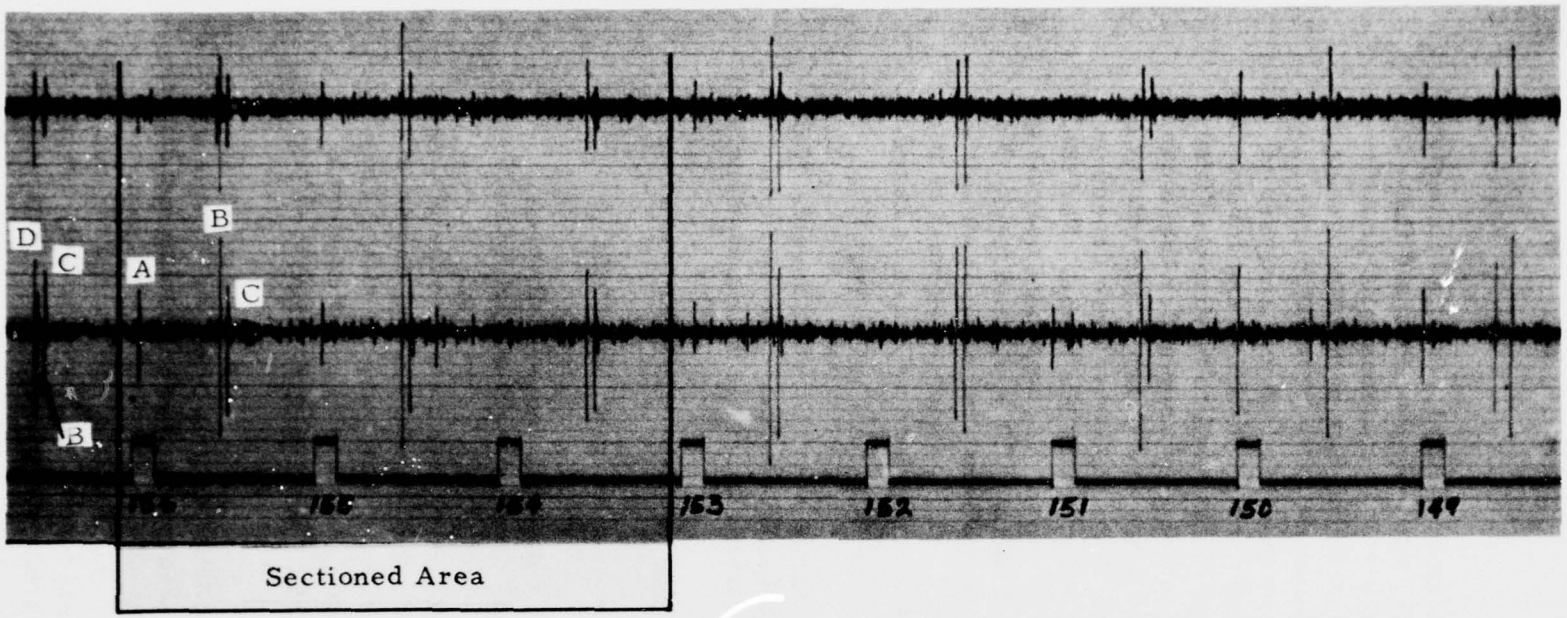

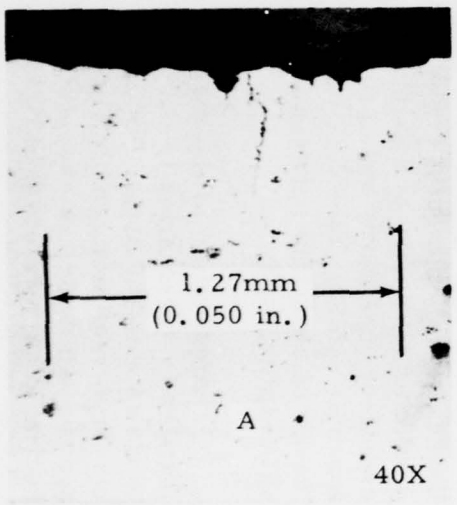

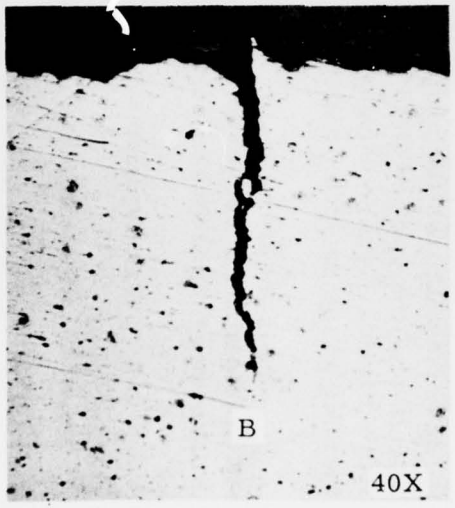

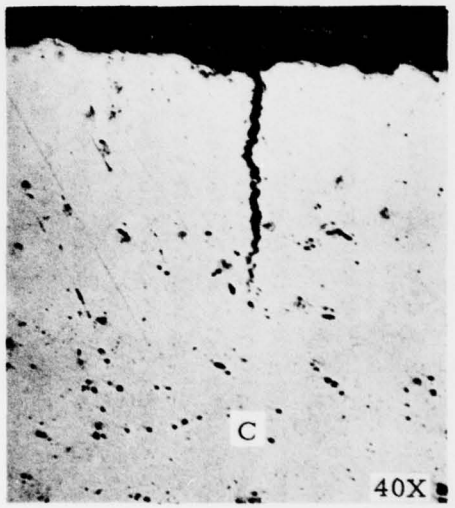

FIGURE 2. SPECIMEN 3, LOT 2-12 INSPECTION RECORD WITH PHOTOGRAPHS OF SECTIONING RESULTS

II. DESCRIPTION OF METHOD

The magnetic perturbation inspection method essentially consists of establishing a magnetic flux in a ferromagnetic material and then scanning the surface of the material with a sensitive magnetic probe to detect anomalies or perturbations caused in the flux by nonhomogeneities in ferromagnetic material. Figure 3 schematically illustrates this concept. Physically, this is a problem in magnetostatics and analyses of solutions have provided guidance for optimizing conditions and forecasting results. In the upper illustrations, flux is assumed to be directed from right to left, and computer plots of signatures obtained under these conditions from nonferromagnetic regions or flaws are shown in the two lower illustrations. The characteristic shape of the signatures are dependent on the magnetic field component which is sensed by the probe. For the upper signatures the probe is oriented to sense the component normal to the applied field and the scan is in the direction of the applied field. For the lower signatures the probe is oriented to sense the component in the direction of the applied field and the scan is in a direction normal to the applied field. Other configurations are possible and selection is based on analysis of the specific inspection of interest.

Analysis of characteristic signatures provides considerable quantitative information concerning the perturbation source. For example, (in the upper signature of Figure 3), quantities that can be derived include:

a) flaw location - coincides with the zero crossing

b) flaw volume - indicated by peak-to-peak amplitude

c) flaw depth from surface - related to the peak-to-peak separation measured in the direction of the applied field

Extensive experimental results show general agreement with many details predicted by theory and also have confirmed that the method provides escellent qualitative and, after calibration, quantitative results. For example, in Figure 4 data obtained from a small fatigue crack show a linear relationship between crack opening displacement, COD, and signal amplitude.

Application of the magnetic perturbation method to the 155mm projectiles is schematically illustrated in Figure 5. For maximum sensitivity to flaws with the major dimension oriented along the axial direction, a circumferential magnetic flux is provided. Under these conditions and with a scan path which is essentially circumferential, but continuously advanced during each revolution (a tight helical scan) characteristic normal component

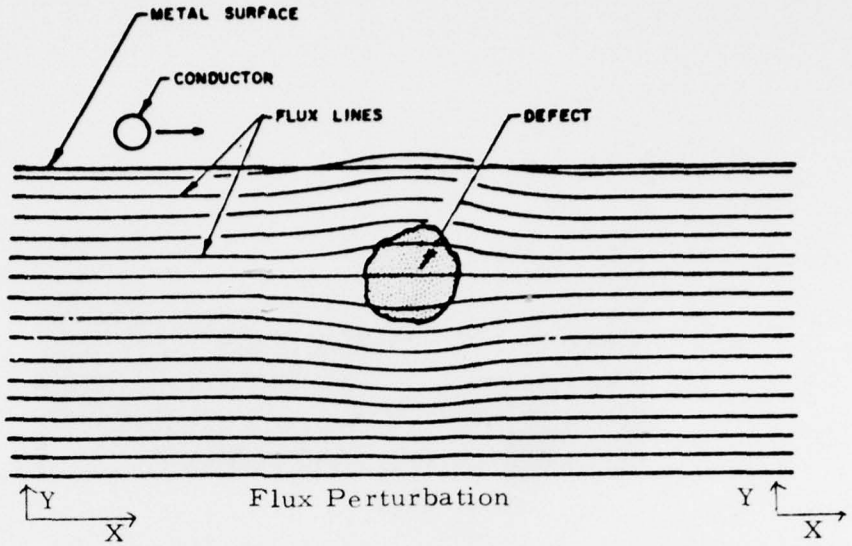

Effect of Inclusion Upon Magnetic Field for Two Depths for an 0.05-in. Inclusion with Applied Field in X-Direction. Scan is in Either X- or Y-Direction.

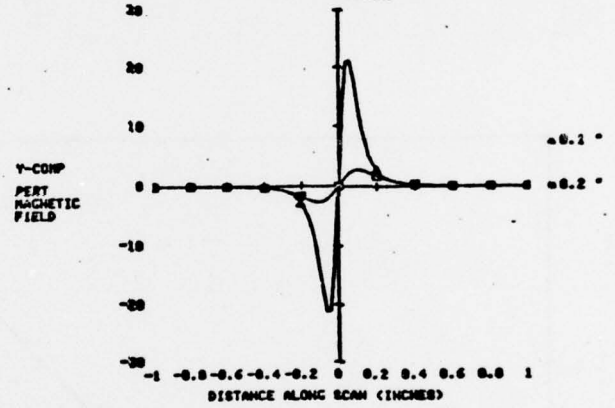

Effect of Inclusion Upon Magnetic Field for Two Depths for an 0.05-in. Inclusion with Applied Field in X-Direction. Scan is in Y-Direction.

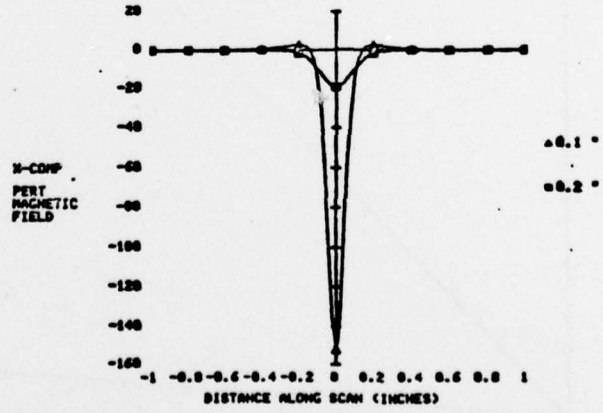

FIGURE 3. SCHEMATIC REPRESENTATION OF MAGNETIC PERTURBATION METHOD AND COMPUTER PLOTS OF SOLUTIONS-SIGNATURES

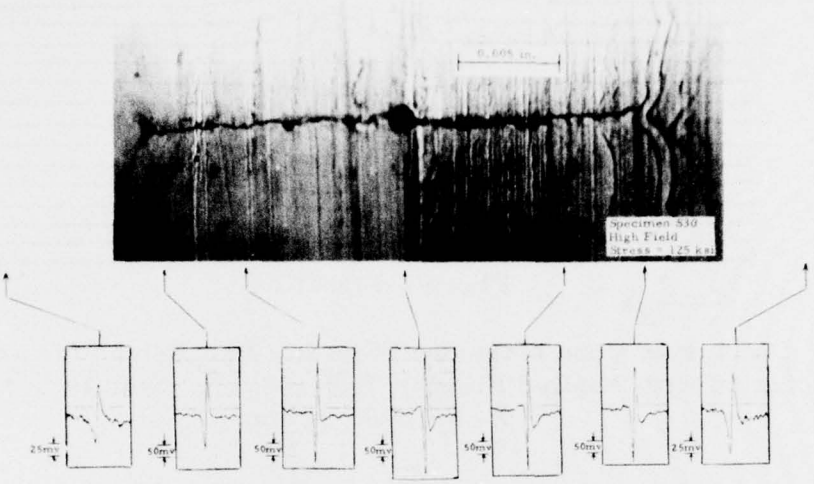

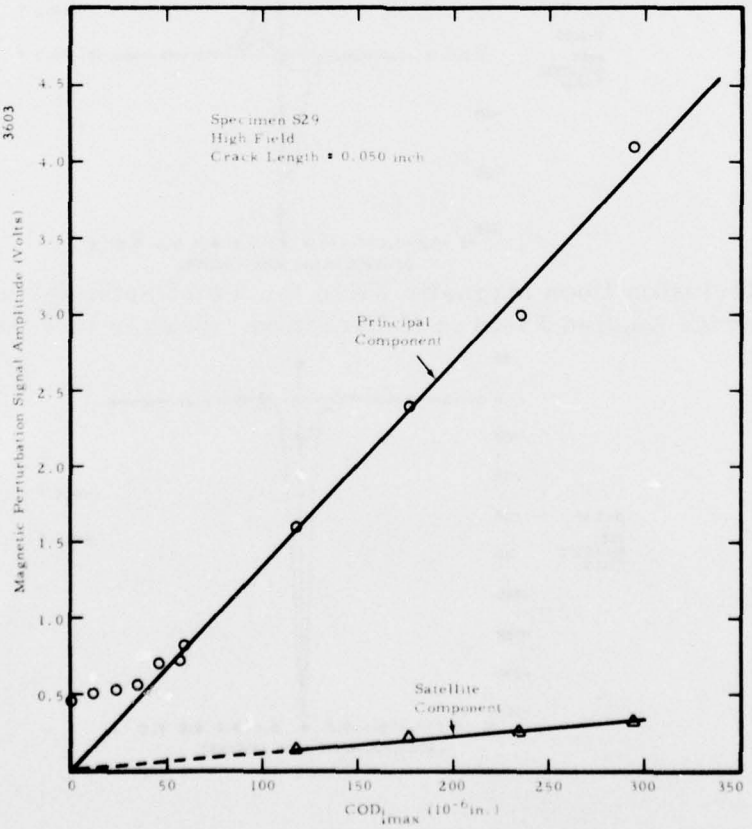

FIGURE 4. FATIGUE CRACK SIGNATURES AND GRAPH OF PRINCIPAL COMPONENT AMPLITUDE VERSUS CRACK OPENING DISPLACEMENT (COD) AT CENTER

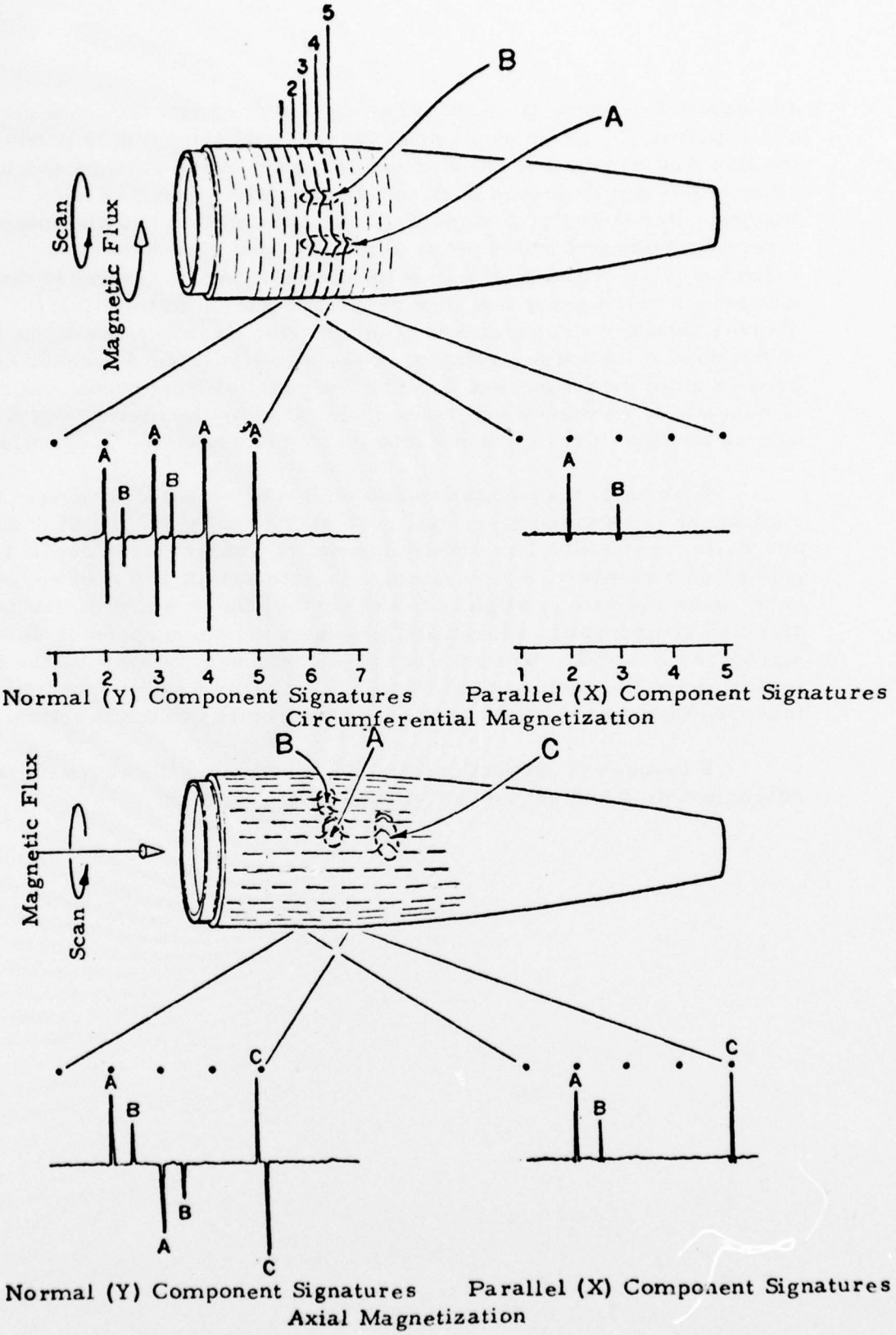

446 i

FIGURE 5. SCHEMATIC SHOWING DERIVATION OF MAGNETIC SIGNATURES

and parallel component signatures obtained from two different size flaws are illustrated. The normal component of magnetic flux is produced by the flaw and on one side the flux is forced out of the surface and on the other side must be forced back into the surface since flux must be continuous. Accordingly, a signature is generated that has an upward directed component which peaks and returns to zero with the zero crossing coincident with the flaw location and then a downward directed component which peaks and then returns to zero. In the illustration signatures obtained on successive scans provide an indication of the length of the flaw in the axial direction. Note that signature A extends over a greater axial direction than B. For the parallel component, the signature is essentially unidirectional and is generated by the increase in flux density as the flaw forces flux out into the region above the projectile surface.

With axial magnetization and the probe oriented to sense the normal component and a circumferential scan path slightly to the left of flaws A and B, the outwardly directed component of flux produced by the flaw generates a signature which rapidly rises to a peak and then returns to zero; when the path is slightly to the right of flaws A and B, the inwardly directed component is sensed and produces the corresponding downward signatures A and B. When the parallel component is sensed, the increase in flux above the surface of the projectile causes a corresponding rapid increase in signature which peaks and then returns to the baseline.

Examples of inspection records illustrating the above signature characteristics and sequences will be reviewed later.

III. ADAPTATION OF INSPECTION EQUIPMENT

As stated in the Introduction, two separate magnetic orientations were used for the inspections. This necessitated tooling and modification of two existing laboratory devices.

A. Circumferential Magnetic Orientation

For the circumferential magnetic orientation, a lathe-type device was modified to provide helical scanning of the projectile surfaces. This was accomplished by designing a carriage to support the magnetic circuit and the probes which could be moved in an axial direction as the projectile was rotated by a modified lathe chuck. Figure 6 shows an overall view of the lathe device and associated instrumentation. A helical scan of 0.1-in./rev. was achieved by using the lead screw on the lathe device. Probe position information was provided through the use of a shaft encoder coupled to the main spindle of the lathe. The magnetizing arrangement consisted of two electric coils with iron cores and return paths, and movable pole pieces. The pole piece design incorporated a four-bar linkage, which together with roller followers in the nose of the pole pieces that roll on the projectile surface, allows the pole pieces to follow the contour of the projectile. In this modified lathe device, it was also necessary to design and fabricate a centering support for the nose of the projectile to counteract the large magnetic forces caused by the magnetizing arrangement. The support was also designed to accommodate insertion of the probes for interior scan of the projectiles. Figures 7 and 8 are close-up views of the pole piece camming operation and the probes at two different locations on the projectile. Figure 9 is a photograph with a cut-out segment of a projectile to illustrate the probe arrangement for scanning the interior surfaces. A rectangular wire coil induction type probe with an orientation to sense the normal component of magnetic flux was designed for the circumferential magnetization arrangement. Previous experience indicated that a coil length of 0.050-in. (1.27mm) would provide high resolution consistent with the contractual requirement for detectability of a minimum flaw size of 0.050-in. (1.27mm) long by 0.015-in. (0.38mm) deep. Two probes, side by side, were used to effectively cover a strip 0.1-in. wide each revolution, thereby permitting a relatively fast axial traverse of the projectile. (Additional instrumentation channels and probes could permit an even wider scan per revolution and a corresponding increase in axial traverse speed.) Rotational speed was approximately 190 rpm and total time to scan the projectile was 45 seconds.

Because of the compound curves encountered on the projectile, it is necessary that a probe-carriage and suspension be designed which will allow the probe to follow the projectile contours while maintaining

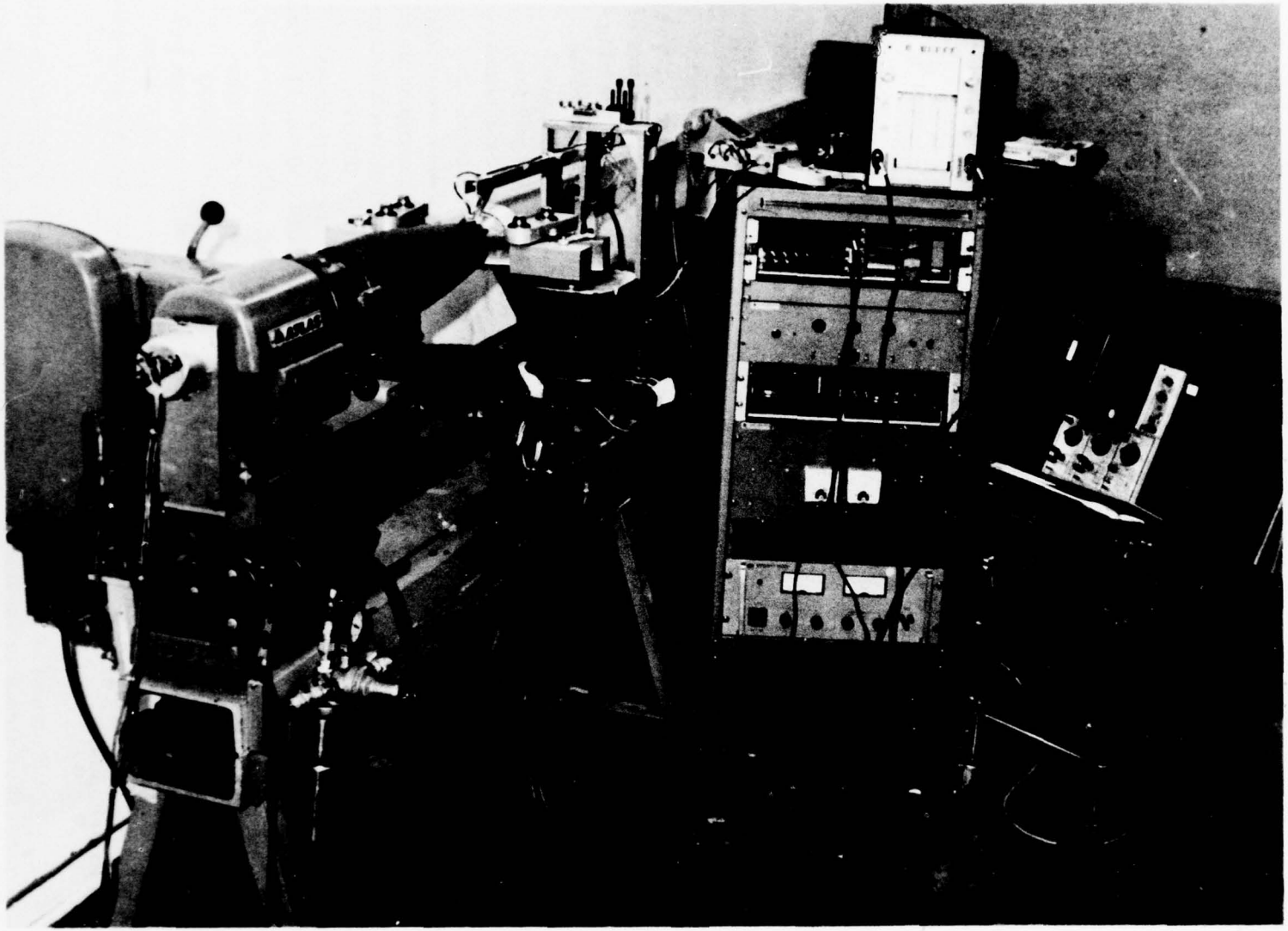

FIGURE 6. OVERALL VIEW OF LATHE DEVICE ADAPTED FOR HELICAL SCAN AND CIRCUMFERENTIAL MAGNETIZATION OF 155mm PROJECTILE

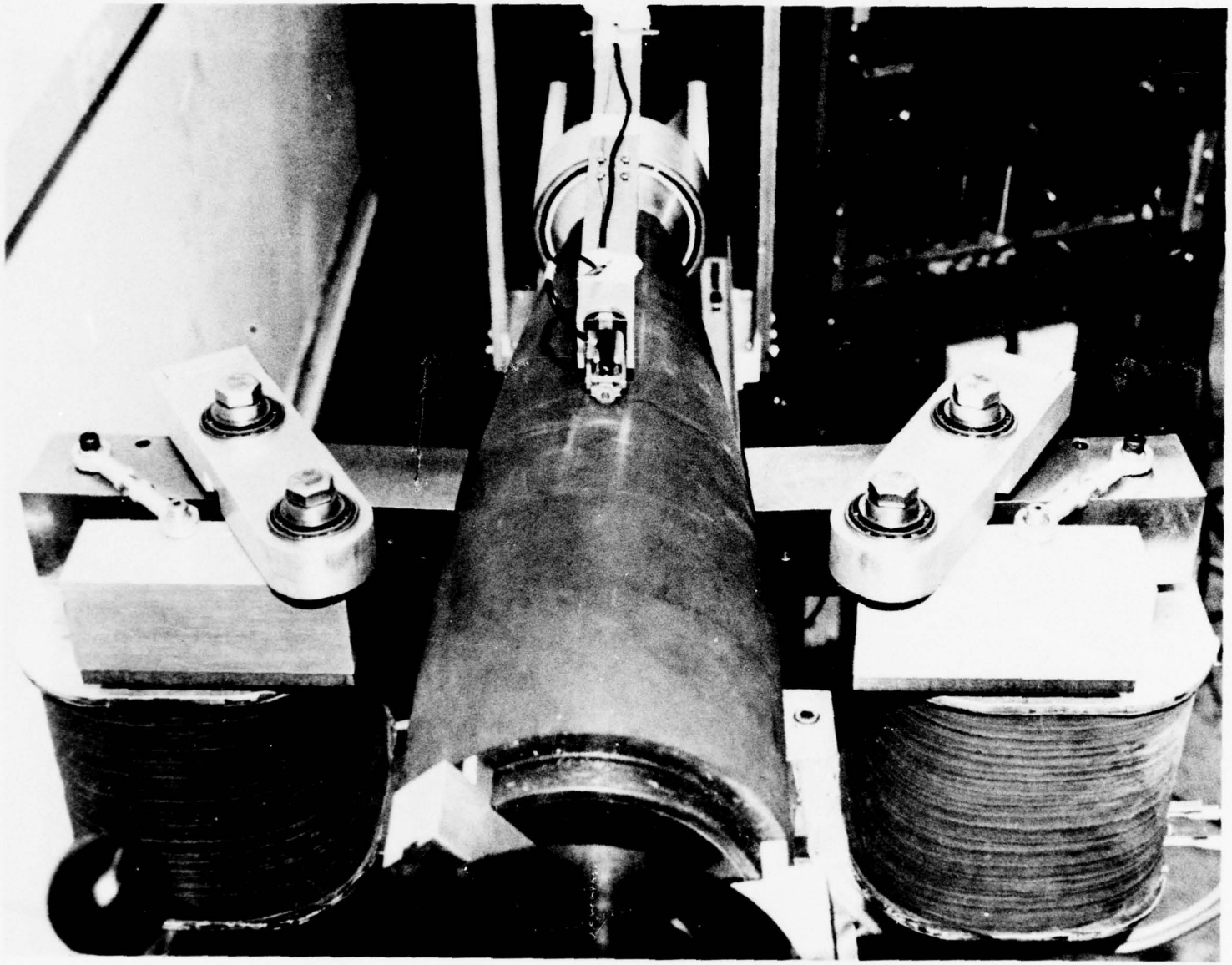

FIGURE 7. LATHE DEVICE SHOWING POLE PIECE LINKAGE MECHANISM

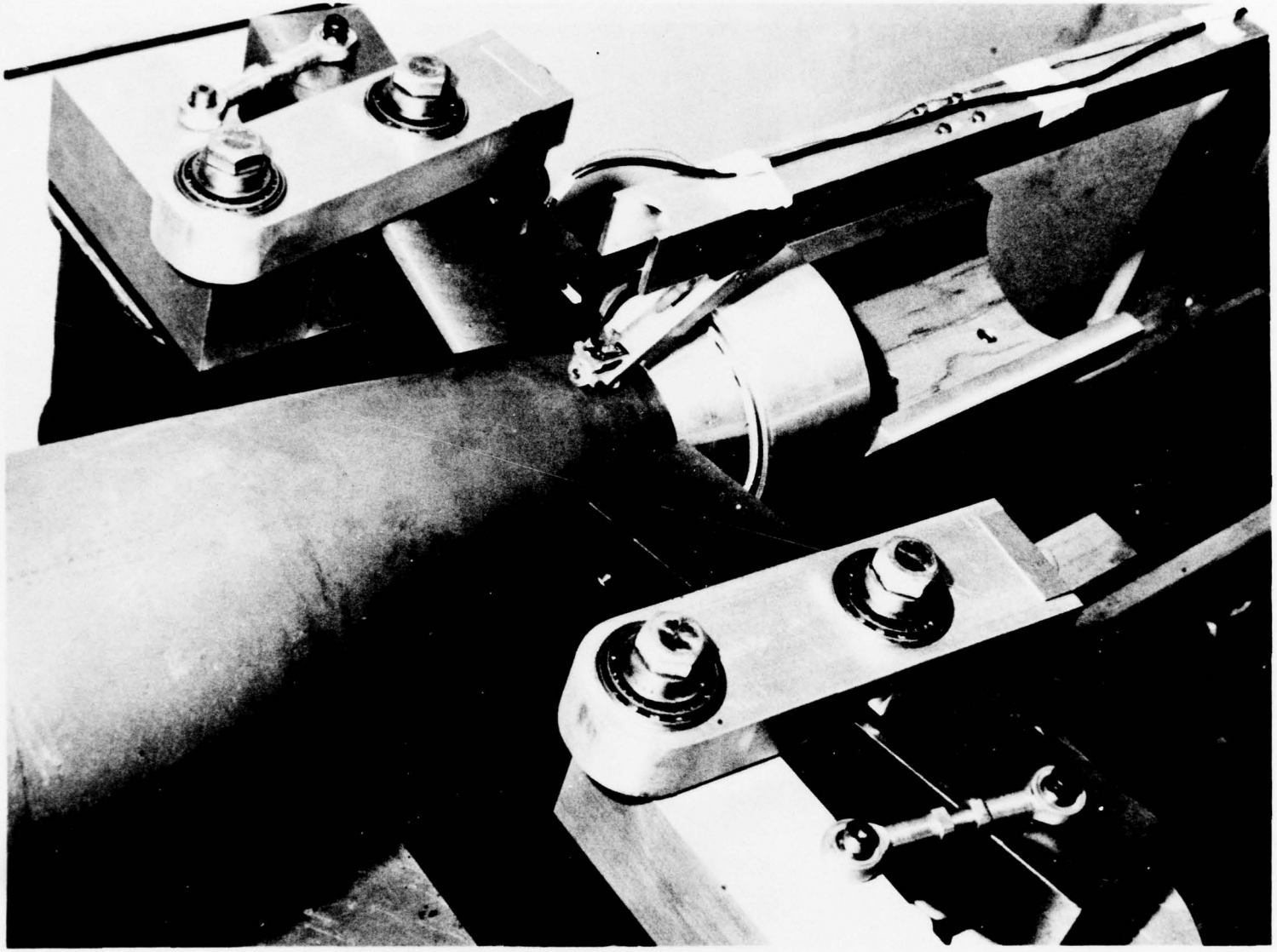

FIGURE 8. LATHE DEVICE SHOWING PROBE MECHANISM FULLY EXTENDED AT NOSE OF PROJECTILE

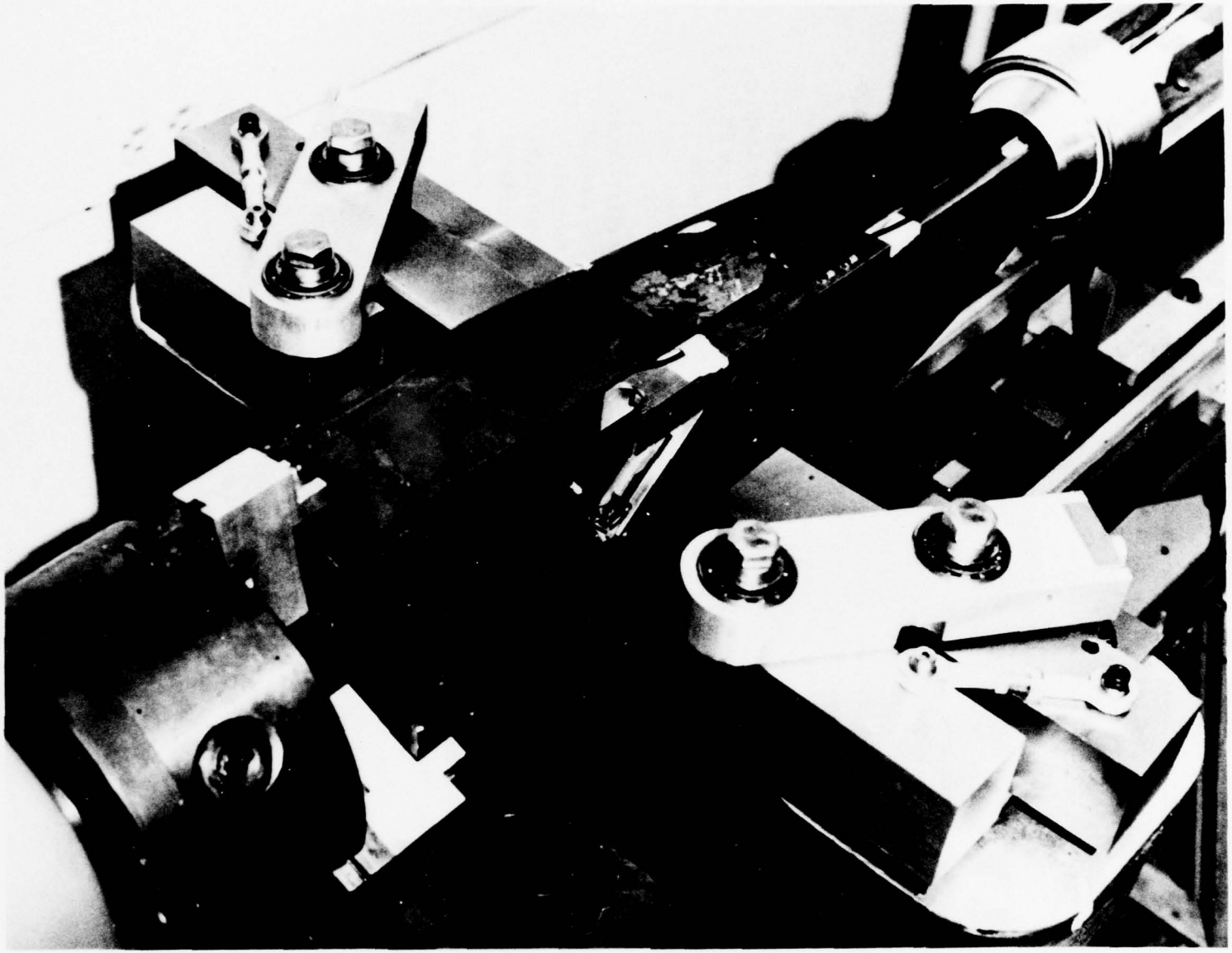

FIGURE 9. LATHE DEVICE SET UP FOR INTERNAL INSPECTION OF PROJECTILES (Cut-away segment to show interior)

close coupling to the surface. Figure 10 shows two views of the probe assembly. In operation, the probe assembly is free to pivot and maintain the assembly parallel with the inspection surface as the contour changes from the base end to the nose end of the projectile.

B. Axial Magnetization

For the axial magnetization orientation, an existing special-design magnetic scanning device was modified to provide for specimen rotation and helical scan. An overall view of the equipment arrangement is presented in Figure 11. Axial magnetization is provided by the encircling electric coil and both the probe and magnetizing coil are fixed with respect to the equipment support structure. The projectile and rotating mechanism are mounted on a carriage supported by ball-bushings and tracks, thereby permitting the projectile to be moved through the magnetizing coil. A complete scan of the projectile is accomplished by synchronizing the rotational speed with the axial motion of the carriage, thereby providing a helical scan. Close-up views showing exterior inspection at two different locations on the projectile are shown in Figures 12 and 13. The same probe-support arrangement is used for the inside inspection (see Figure 8).

Probe design for the axial magnetization using helical scan required a different probe coil orientation than was used in the case of circumferential magnetization. The coil was oriented with the axis parallel to the projectile and magnetization axis and therby sensed the magnetic field component which was parallel to the projectile surface. With this configuration it was necessary to use five side-by-side coils to cover a scan path 0.1-in. wide/rev. This probe arrangement resulted in excellent sensitivity to transversely oriented flaws in the size range of interest.

C. Base Region

Figure 14 is a photograph of the arrangement for inspecting the outside surface of the base region. With this arrangement the projectile is rotated and the probe is moved across the base causing a spiral scan. Movement in the horizontal direction and then in the vertical direction provides a method for examining flaws in flux orientations approximating two directions over much of the base. A Hall-effect probe is used to eliminate the influence of velocity on the signatures.

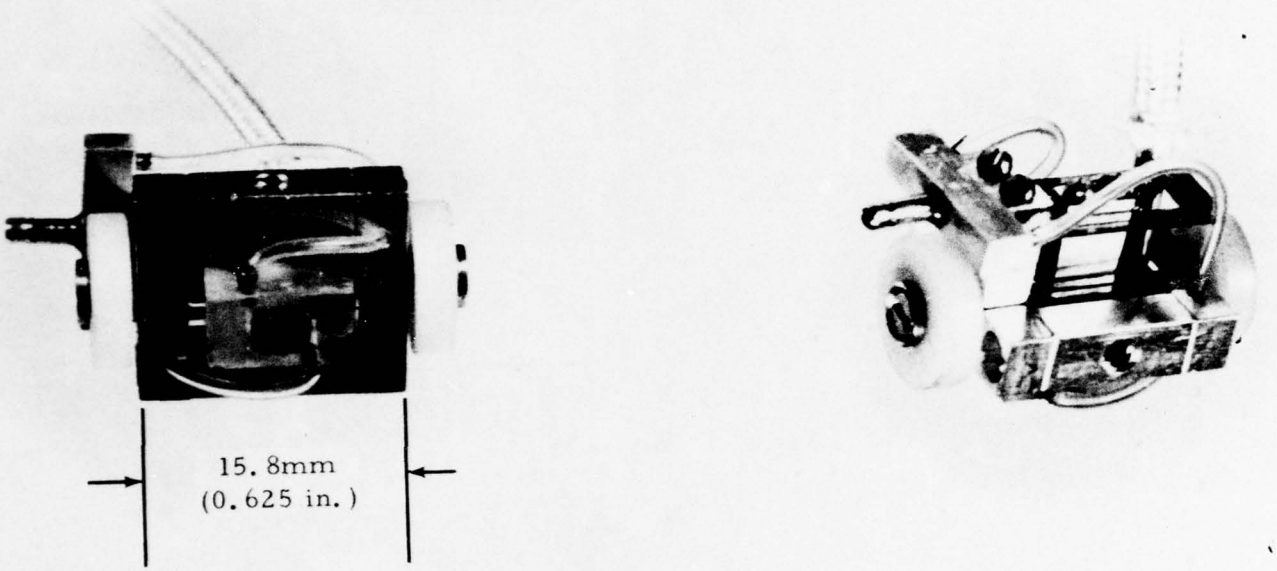

FIGURE 10. PROBE CARRIAGE WITH PROBE AND PROBE SUSPENSION INSTALLED
(Note, manifolds for air cushion coupling)

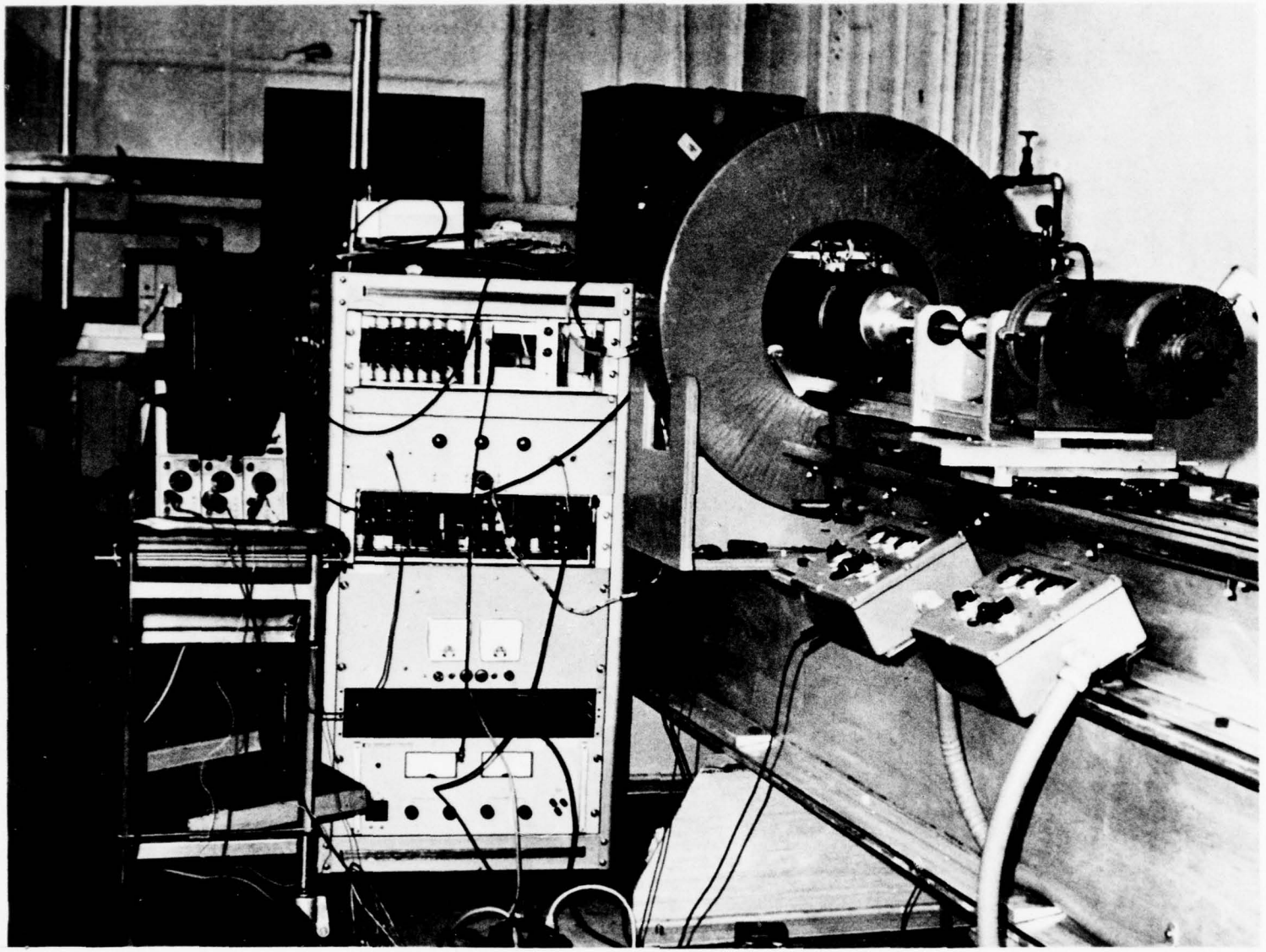

FIGURE 11. OVERALL VIEW OF LONG BED AXIAL MAGNETIZATION DEVICE

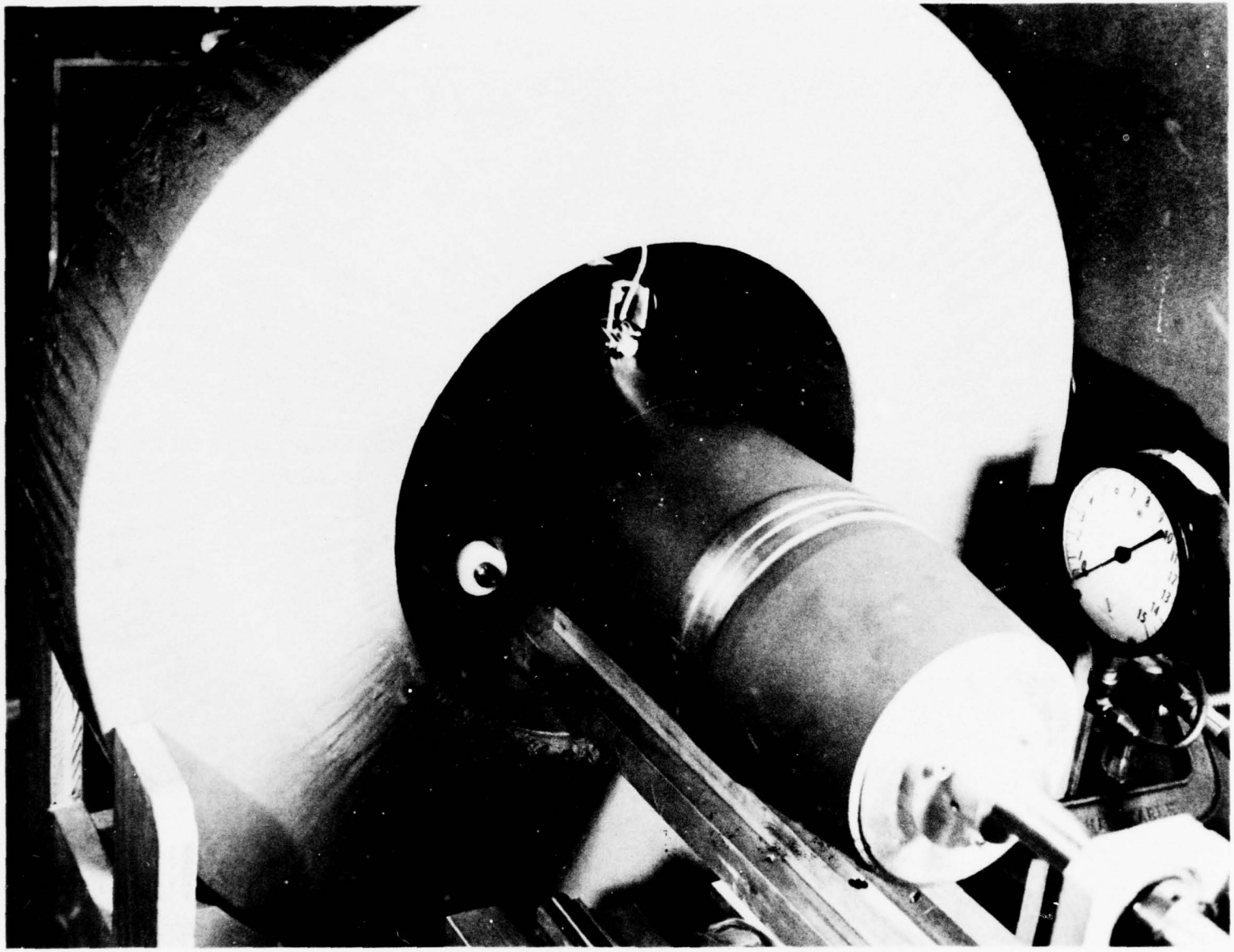

FIGURE 12. PROBE CARRIAGE IN BOURELLET SECTION (Long Bed Device)

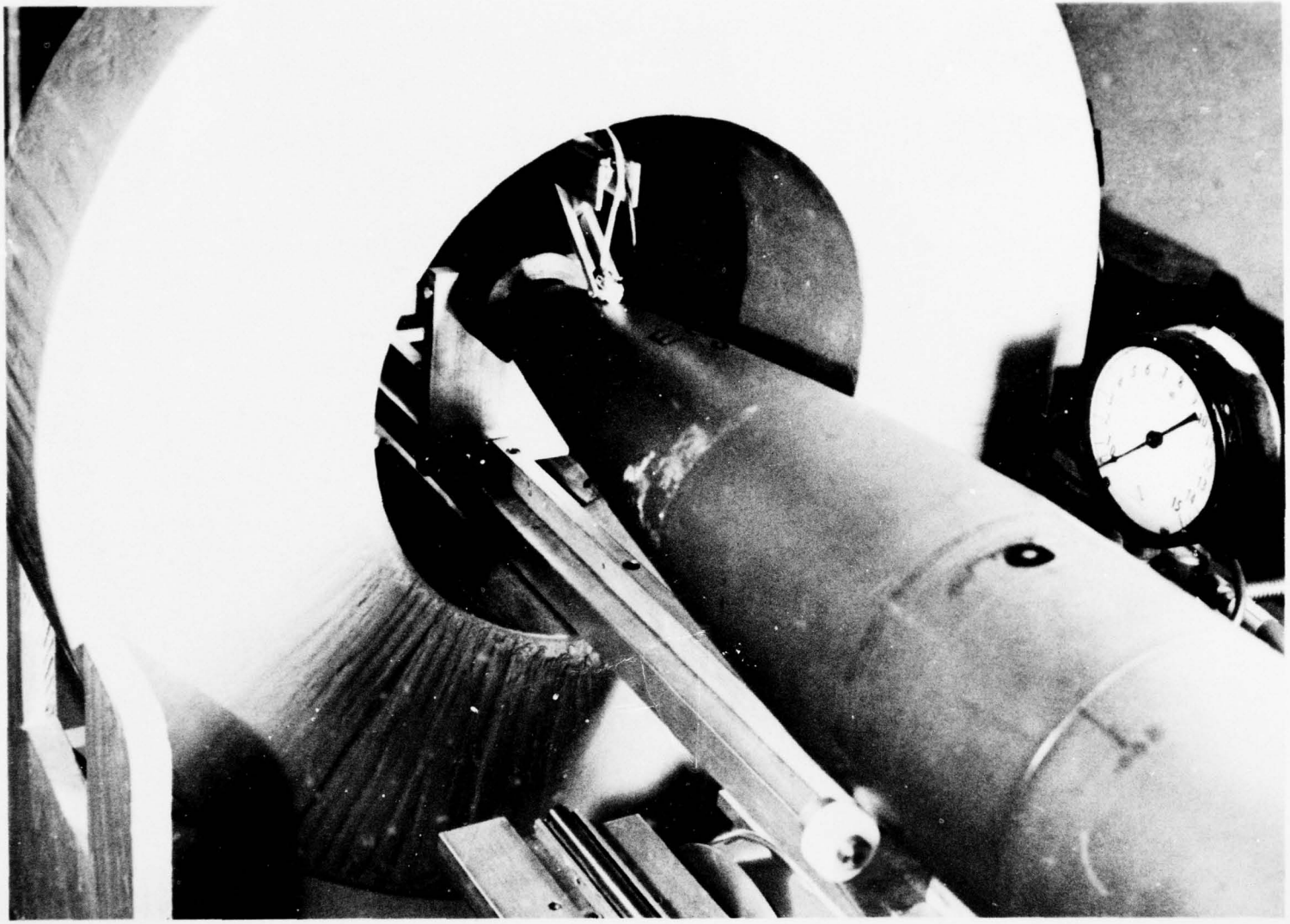

FIGURE 13. PROBE CARRIAGE IN OGIVE AREA (Long Bed Device)

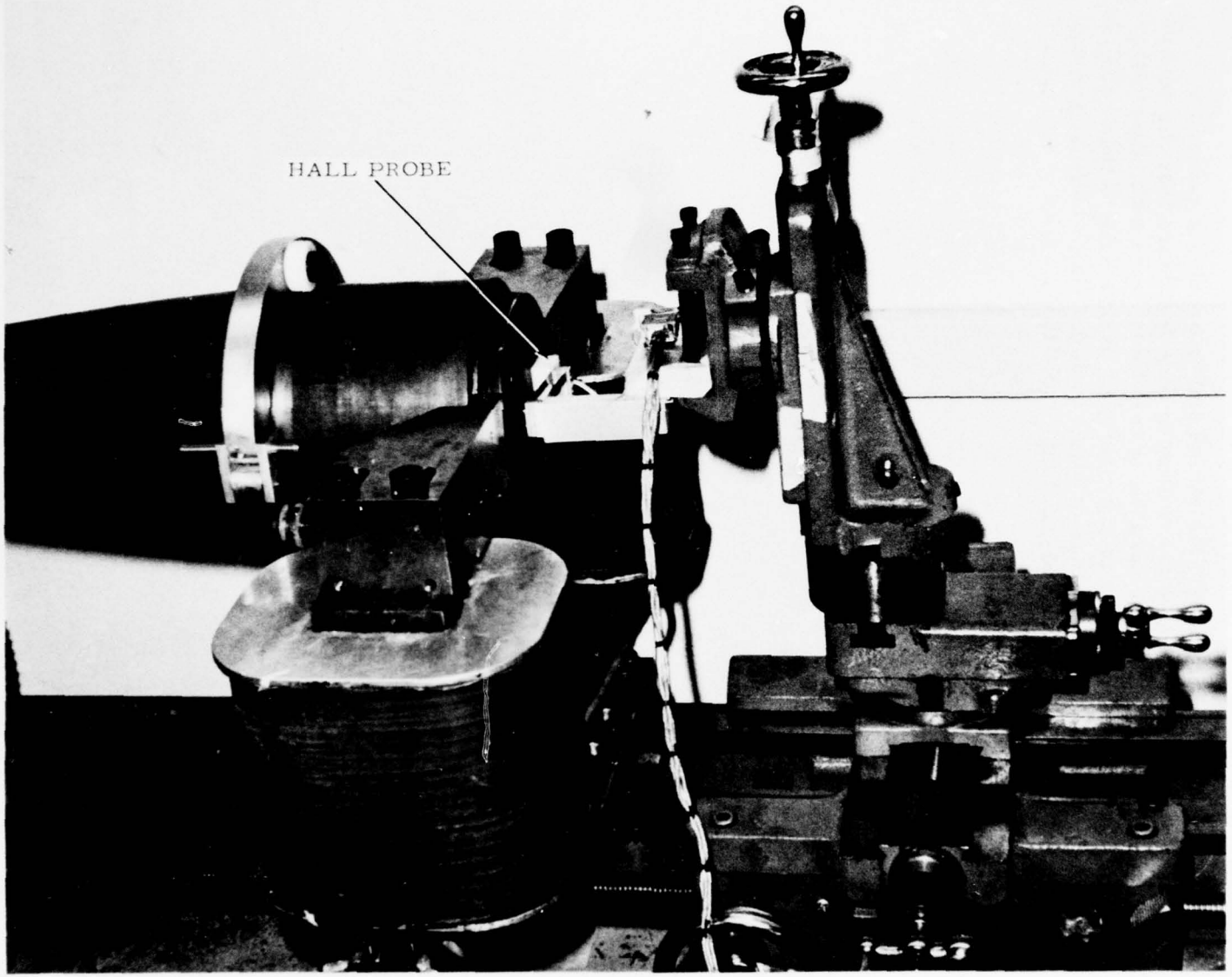

FIGURE 14. SETUP FOR EXTERIOR BASE INSPECTION

D. Reference Specimen

For preliminary evaluations and to provide a reference specimen which could be used from time to time to ensure that the equipment was operating properly, targets or test flaws were machined in the exterior and interior surfaces of a projectile. A schedule of these defects is shown in Figure 15. The range of sizes included flaws both larger and smaller than the specified 0.050-in. long by 0.015-in. deep.

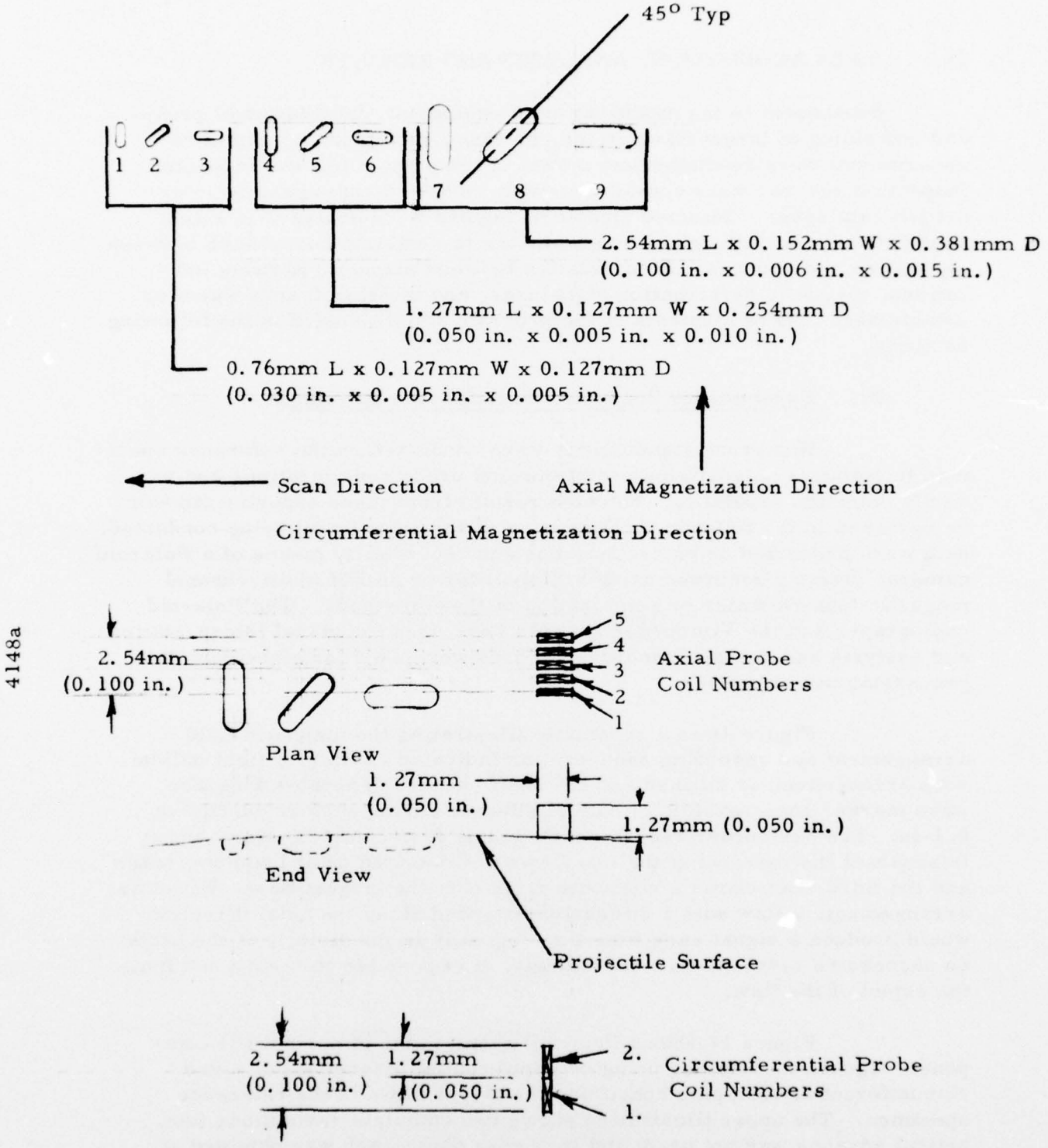

FIGURE 15. DEFECT SCHEDULE AND ORIENTATION

IV. DATA ACQUISITION, ANALYSES AND RESULTS

Subsequent to the modification of equipment, fabrication of probes and machining of target flaws in the reference specimen, a number of experiments were conducted and a total of ten projectiles was inspected. Inspection records were comprehensively reviewed and signature information catalogued. Selected signature regions were analyzed to select candidates for metallurgical investigations to establish correlation between signatures and sources. A correlation between magnetic particle indications, magnetic perturbation signatures, and interior cracks was also established. These elements of the program are presented in the following sections.

A. Experiments Conducted on Reference Specimen

Numerous experiments were conducted on the reference specimen to optimize magnetizing conditions and probe configurations and to verify detection capability. Selected results from these experiments will be reviewed in the following. Depending on the experiment being conducted, data were presented on an oscilloscope and recorded by means of a Polaroid camera, directly recorded using a Visicorder or an FM multi-channel magnetic tape recorder or combination of these methods. The Polaroid photographs and the Visicorder records were used for visual interpretation and analysis and the tape recorder records were used for electronic data processing investigations.

Figure 16 is a schematic illustrating the magnetic field arrangement and recording sequence; as indicated earlier, a tight helical scan arrangement is utilized and the shaft encoder generates a square wave marker each revolution; helical advance during each revolution is 0.1-in. The Visicorder record shows nearly four complete scans and it is apparent that several of the test flaws are detected on at least two scans and the third scan shows a signature from only the largest flaw. With this arrangement, a flaw with a dimension extended along the axial direction would produce a signal each time that region is in the vicinity of the probe on successive revolutions. Accordingly, it is possible to readily estimate the extent of the flaw.

Figure 17 shows Polaroid photographs of normal (Y) component signatures obtained using circumferential magnetization and a circumferential scan path containing the target flaws in the reference specimen. The upper illustration shows two complete revolutions (the helical advance was not used) and the lower photograph was obtained at an expanded horizontal sweep to reveal the characteristic signature features. (This is configuration A of Figure 5.) The largest signatures are

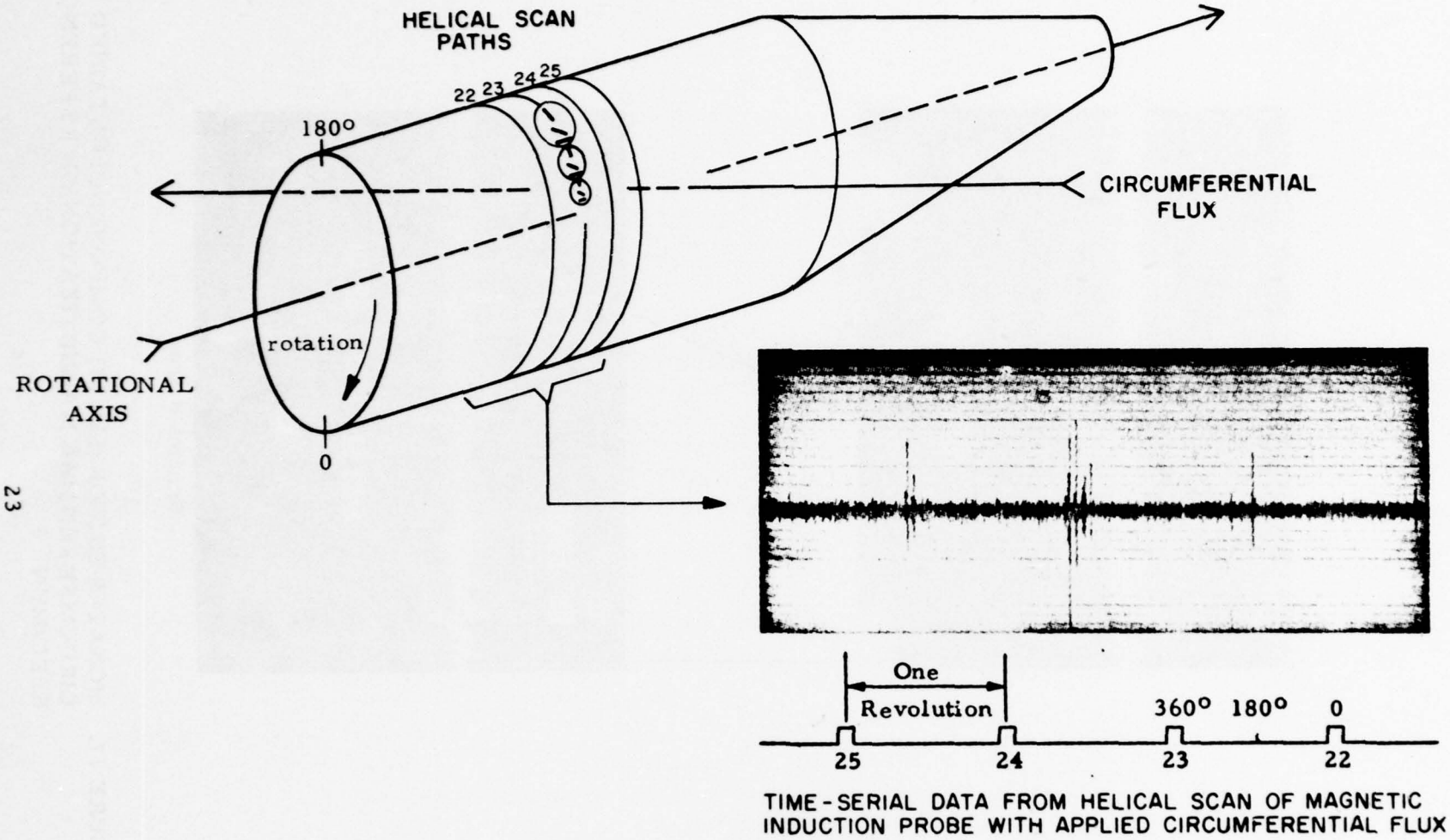

FIGURE 16. SCHEMATIC, ILLUSTRATING MAGNETIC FIELD ARRANGEMENT AND RECORDING SEQUENCE

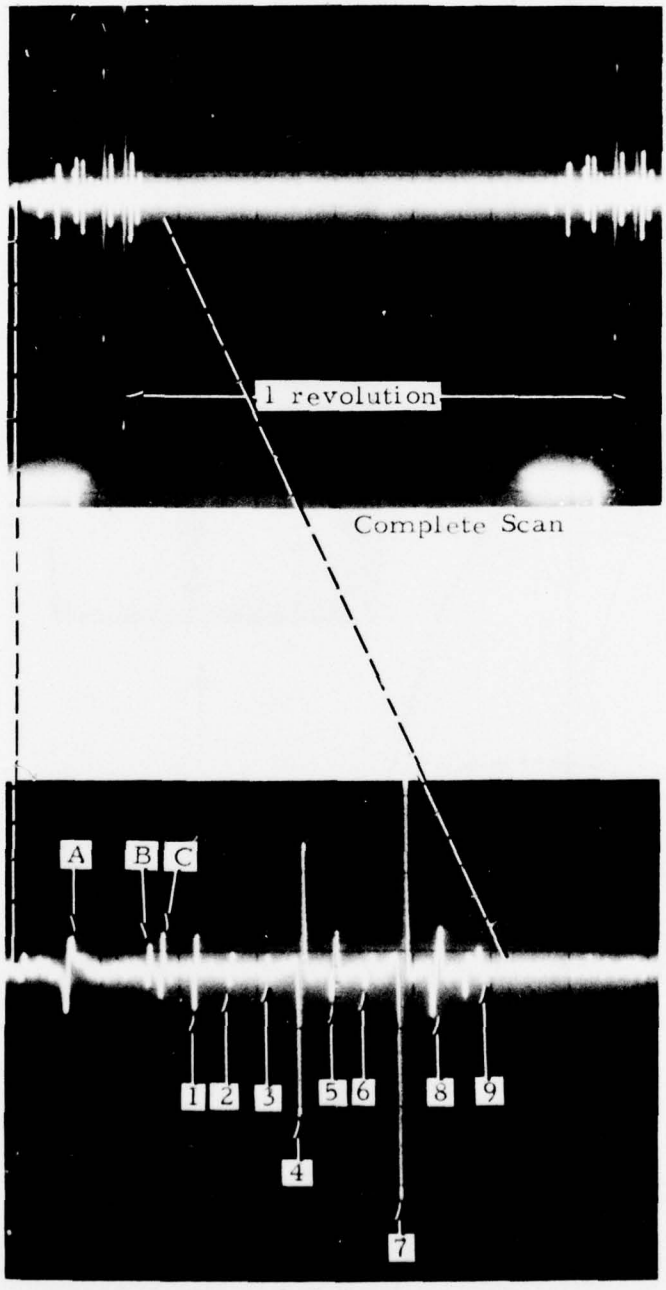

4462

FIGURE 17. SIGNATURES (NORMAL (Y) COMPONENT) OBTAINED USING CIRCUMFERENTIAL MAGNETIZATION ON REFERENCE SPECIMEN

obtained from flaws 1, 4 and 7, since these are oriented with the major dimension perpendicular to the flux. Flaws 2, 5 and 8 which are oriented at an approximate angle of 45° to the flux direction produced significantly lower signal amplitudes and also the peak separation is more extended than for the flaws 1, 4 and 7. For flaws 3, 6 and 9, oriented at 90° to the flux, signature amplitude is markedly reduced and peak separation is greatly exaggerated compared to the normally oriented flaws. Visicorder records from the two side-by-side coils produced by the same series of flaws are shown during a spiral scan in the lower records of Figure 18. Note the change in relative signal amplitudes from specific flaws as the spiral scan progresses. The upper records show signatures from a sequence of target flaws fabricated into the interior surface of the reference specimen. Polaroid records showing normal (Y) component signatures from the target flaw sequence with axial magnetization and a circumferential scan (configuration C of Figure 5) are presented in Figure 19. In this case the largest amplitude signatures are obtained from the flaws oriented at 45° to the magnetic flux and the scan path. Note for flaws oriented parallel to the flux direction that the signature polarity reverses, depending on which side of the flaw the scan path traverses. This is apparent by comparing the signatures on probe coil 1 with probe coil 2 obtained from target flaws 1, 3, 4, 6, 7 and 9.

Horizontal (X) component signatures obtained from the target flaws using axial magnetization are presented in Polaroid photographs and Visicorder records respectively in Figures 20 and 21 (configuration D of Figure 5).

B. Projectile Inspections

A total of ten projectiles were provided by the Government for use on this program. These specimens were part of a group previously inspected ultrasonically and rejected at the Iowa Army Ammunition Plant. Accordingly, it was anticipated that most of the projectiles would contain one or more flaws. Eight of the ten projectiles were inspected on both the exterior and interior Bourellet and Ogive surfaces, while two, specimen Nos. 19 and 40, Lot 2-9A, were inspected on the exterior surfaces only. Visual examination indicated that these two specimens contained large, sharp projections on the interior surfaces which could possibly have damaged the probes in the present configuration.

For the circumferential flux orientation, two data channels were used and one channel was used for probe position information provided by the shaft position encoder. For the axial flux orientation, five inspection data channels were used and one channel for probe position information.

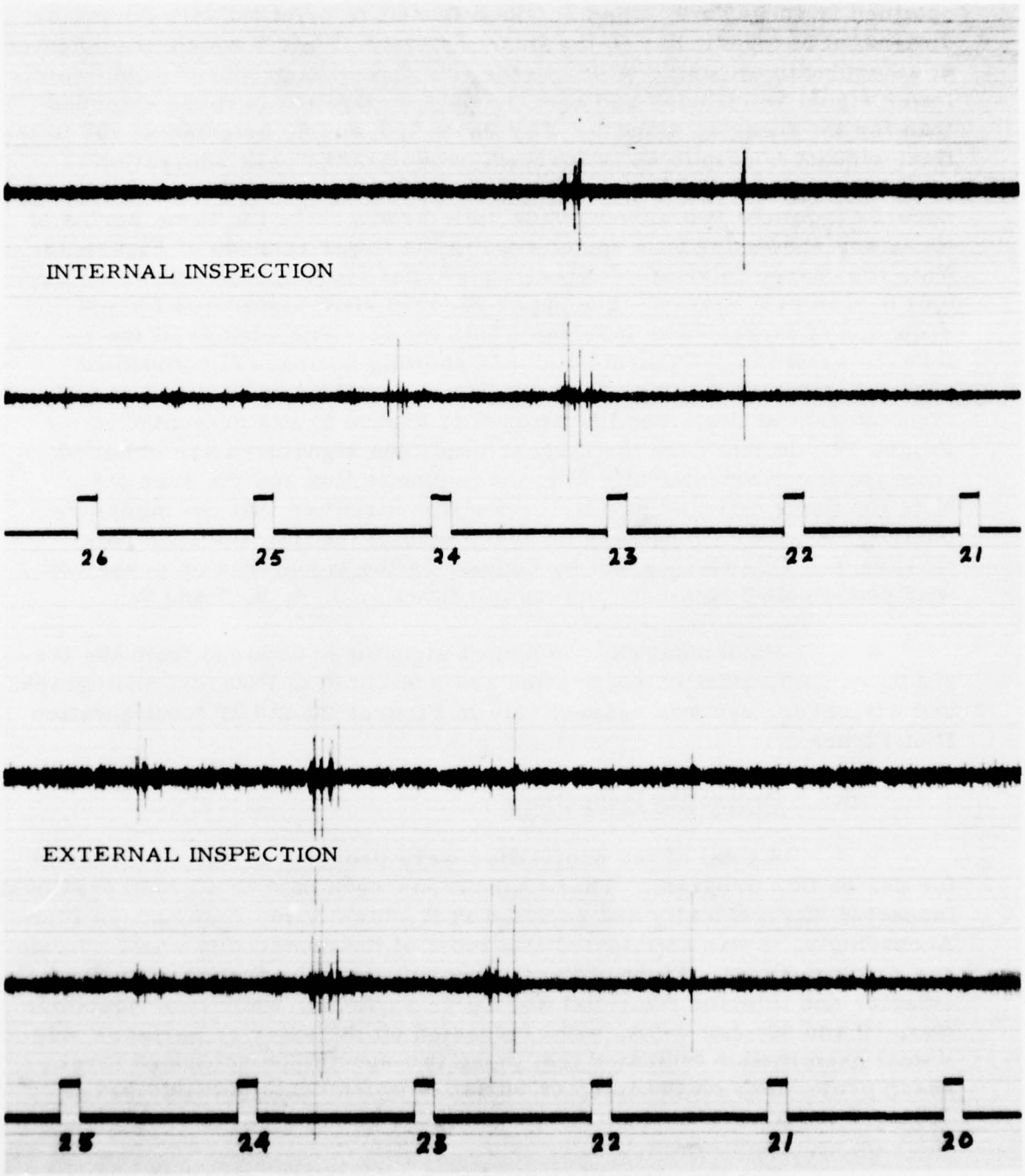

4396

FIGURE 18. STANDARD SPECIMEN (Circumferential Magnetization)

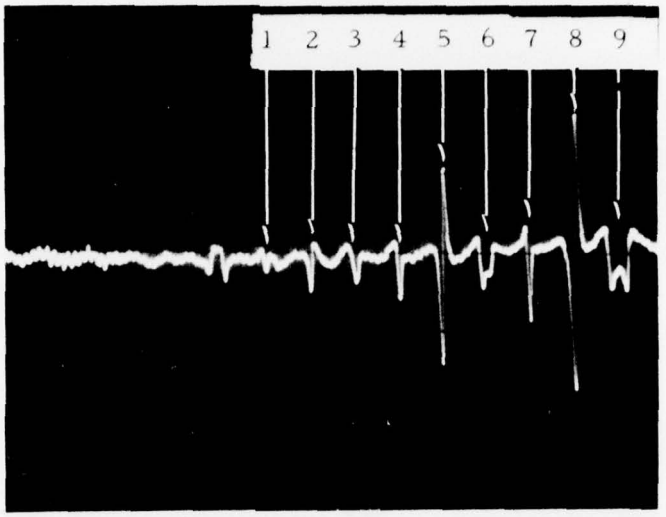

Probe Coil #1

4463

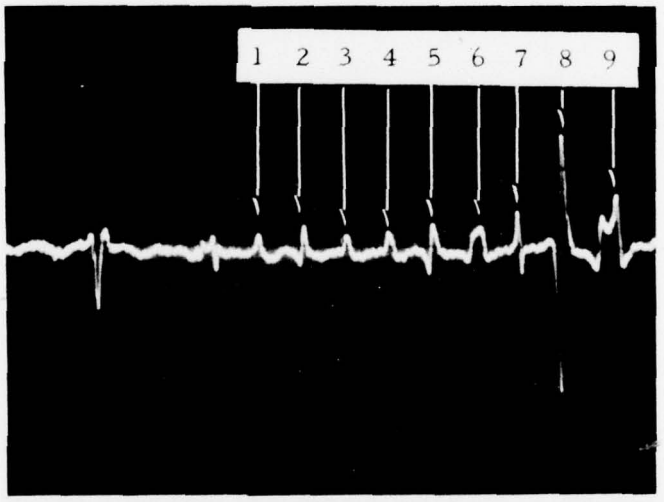

Probe Coil #2

FIGURE 19. AXIAL MAGNETIZATION - NORMAL (Y) COMPONENT SIGNATURES OBTAINED FROM REFERENCE SPECIMEN (Two coil probe)

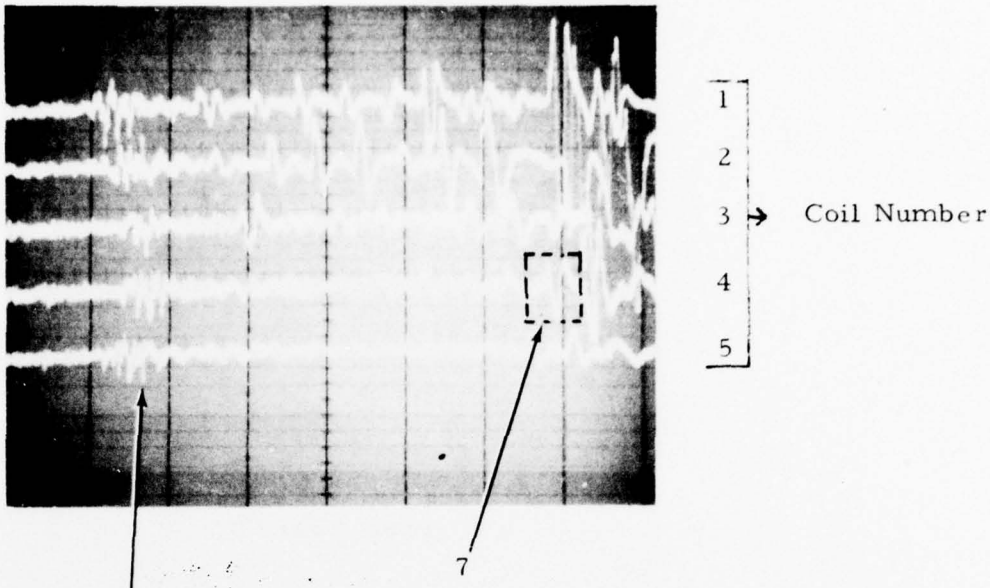

FIGURE 1a.
Composite Scan, All Coils

(a)

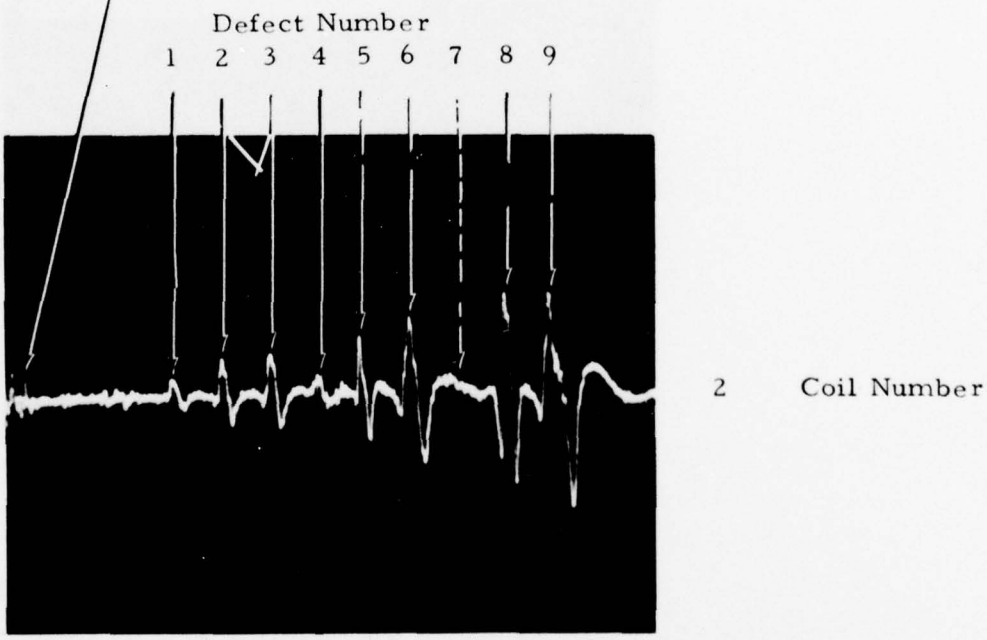

4147

FIGURE 1b.
Coil #2 Scan

FIGURE 20. AXIAL MAGNETIZATION-PARALLEL (X) COMPONENT SIGNATURES OBTAINED FROM REFERENCE SPECIMEN (Five Coil Probe)

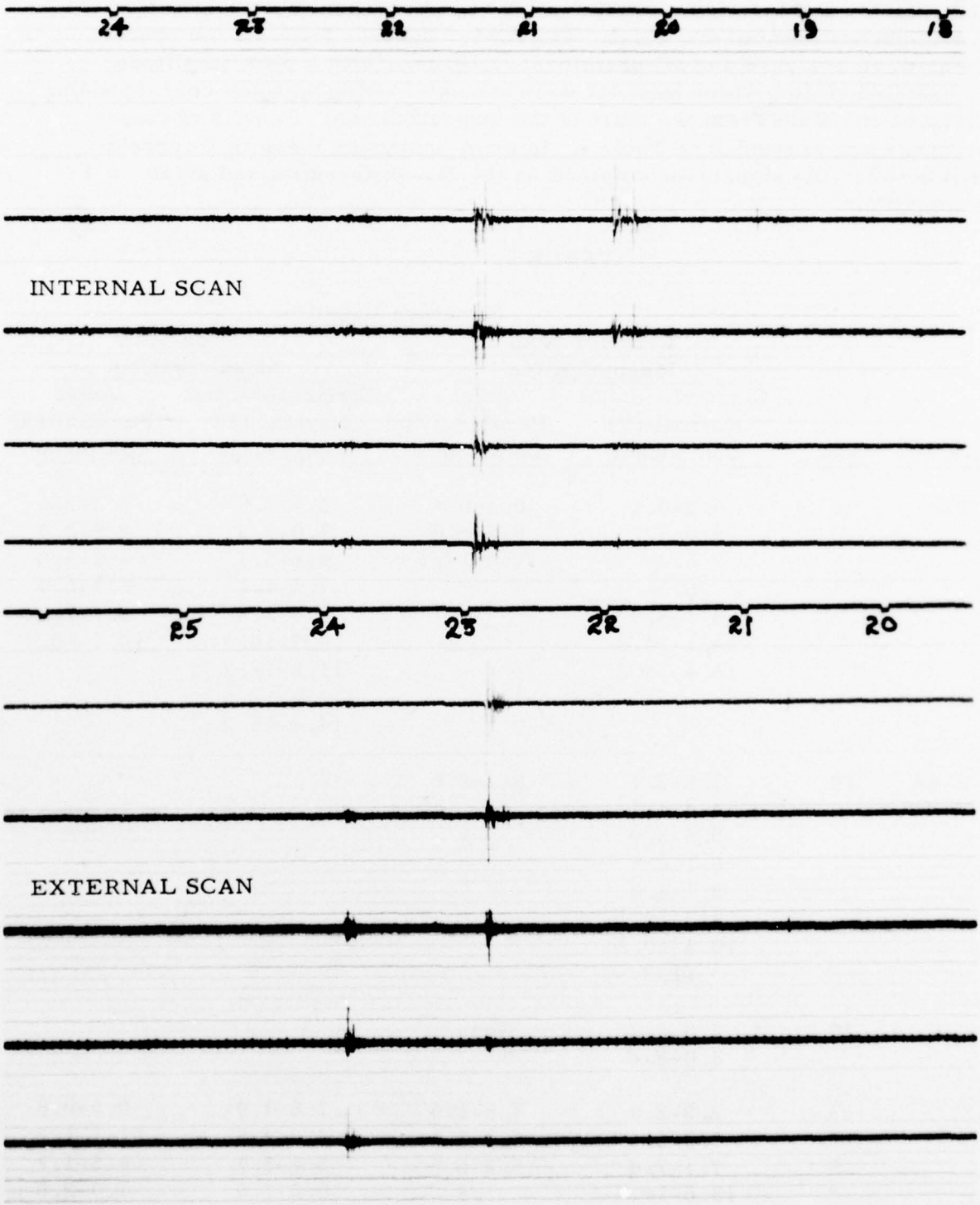

FIGURE 21. STANDARD SPECIMEN (Axial Magnetization)

In most cases, numerous signatures were obtained from the exterior and interior surfaces under each condition of magnetization, i.e., circumferential and axial. Visicorder records from all ten specimens were analyzed and all prominent signatures with a peak amplitude to baseline ratio greater than 3:1 were tabulated along with the corresponding distance in inches from the start of the inspection run. Results of these analyses are presented in Table I. In many instances there is a correlation between the signatures obtained on the circumferential and axial orientations.

TABLE I

		Signature Location			
		Exterior Scan		Interior Scan	
		Magnetization		Magnetization	
Lot No.	Spec.	Circumferential Normal (Y) Component	Axial Parallel (X) Component	Circumferential Normal (Y) Component	Axial Parallel (X) Component
2-8	16	0.2-0.4	0.3-0.4	2.5-2.8	2.3-2.6
	"	5.0-5.7	5.2-5.8	3.0-3.2	2.8-3.0
	"	6.2	16.0-17.1	4.8-5.1	4.8-5.8
	"	6.5		7.3-7.7	6.3-6.4
	"	8.1-8.3		8.4-8.8	6.7-7.5
	"	14.1-14.2		9.9-10.4	10.1-10.3
	"	15.4-16.2		11.8-12.2	
	"			12.3-12.6	
	"			14.4-15.2	
2-9A	19	1.9-2.1	8.2-8.6		
		4.4-4.7			
		5.5-5.9			
		6.1-6.5			
		8.1-8.9			
		9.7-10.1			
		10.5-10.8			
		11.2			
	40	2.0-2.2	None		
		8.0-End			
	3	2.0-2.8	1.5-1.6	1.8-1.9	0.5-0.8
	"	5.9-6.4	5.4-5.6	4.2-4.5	1.1-1.2
	"	7.1-7.4	5.7-6.8	5.6-5.7	1.6-1.7
	"	13.6-14.5	7.8	6.0-7.0	1.9-2.0

		Signature Location			
		Exterior Scan		Interior Scan	
		Magnetization		Magnetization	
Lot No.	Spec.	Circumferential Normal (Y) Component	Axial Parallel (X) Component	Circumferential Normal (Y) Component	Axial Parallel (X) Component
2-12	3			8.5-8.8	2.2-5.0
	"			10.6-11.9	5.6-8.6
	"			12.1-15.4	8.8-10.3
	"				10.5-10.7
	"				12.1-15.4
	10	0.8-1.0	1.2-1.7	2.1-2.2	3.5-4.0
	"	3.5-4.5	3.6-4.1	2.4-2.6	4.1-4.4
	"	10.0-10.6	4.8-4.9	3.6-3.7	6.0-6.3
	"	11.3-11.7	11.5-11.6	10.3-10.4	6.9-7.3
	"	14.0-17.2	13.2-13.6	11.0-11.2	9.7-9.8
	"		14.9	12.7-13.1	10.4-11.8
	"			14.3-14.4	12.0-13.0
	30	2.3-2.8	No	6.1-6.7	4.2-4.6
	"	6.0-6.3	Outstanding	11.0-11.6	8.5-8.9
	"	7.1-7.4	Signals	14.8-15.4	11.3-12.0
	"	8.2-9.7			
	"	13.6-14.4			
	"	15.6-16.4			
2-14	25	1.6-1.7	5.8-6.3	Too numerous to catalog both circumferential and axial	
	"	3.3-4.3	15.2-15.3		
	"	4.0-4.2			
	"	15.1-15.3			
	33	1.2-1.3	No	1.4-1.5	1.3-1.4
	"	4.1-4.2	Outstanding	2.7-3.9	2.2-2.6
	"	9.0-9.1	Signals	4.1-5.8	2.8-3.8
	"	10.7-10.8			
	"	12.9-13.0			
	"	17.1-17.2			
	35	No outstanding signals except broad, low amplitude signal from 10.0 to end of run	5.5-5.9	7.1-7.3	0.3-0.5
	"			7.7	2.4-3.0
	"			8.3	3.3-3.9
	"			9.8	4.6-4.9
	"			14.8-15.0	6.4-6.6
					7.2-8.2
					10.4-10.7

		Signature Location			
		Exterior Scan		Interior Scan	
		Magnetization		Magnetization	
Lot No.	Spec.	Circumferential Normal (Y) Component	Axial Parallel (X) Component	Circumferential Normal (Y) Component	Axial Parallel (X) Component
2-14	37	3.0-3.1	4.2-4.3	15.3-15.4	Mostly broad cyclic signals from beginning to end of run. Probable material anomalie.
	"	3.9-4.1	5.5-5.9		
	"	8.2	6.1-6.2		
	"	8.2 to end	8.4-8.5		
	"	broad signal with			
	"	maximum amplitude between 15.4-16.9			

Subsequent to cataloguing the foregoing data, Specimens 3, 10 and 30, Lot 2-12, were selected as candidates for metallurgical sectioning, because of the wide range of defect signature sizes obtained from these specimens during the inspections. Since analyses indicated the most prominent signatures from the inspections obtained with circumferential magnetization normal (Y) component conditions, most of the sectioning candidates were from such signatures. These three specimens were re-inspected at selected locations to more completely categorize the defect signatures and were marked for sectioning at a total of 12 candidate sites. of the 12 selected candidate sites which were extensively examined magnetically, seven locations were investigated metallurgically, one location by plastic replication, and four by magnetic particle to establish possible correlation between signatures and flaws. In each instance, either an inclusion, metallurgical anomaly, or crack was revealed.

C. Metallurgical Sectioning Investigations and Other Correlations

Two signature regions from Specimen No. 30 were investigated. One of these signatures occurred in the Bourellet section between 2.1 and 2.9 inches from the start of the exterior inspection run. Segments of the records from the two side-by-side coils obtained with circumferential flux normal (Y) component inspections are shown in Figure 22 along with a photograph of the metallurgical sectioning results. An analysis of the upper record shows a small signature at approximately 2.8-in., increasing to a large amplitude signature at 2.7 and 2.6-in., then gradually decreasing to a small signature at 2.2-in. Metallurgical investigation disclosed a stringer type inclusion located approximately 0.015-in. below the exterior surface and extending axially for approximately 0.25-in. This stringer probably extends somewhat more than shown in the photograph based on extent of the

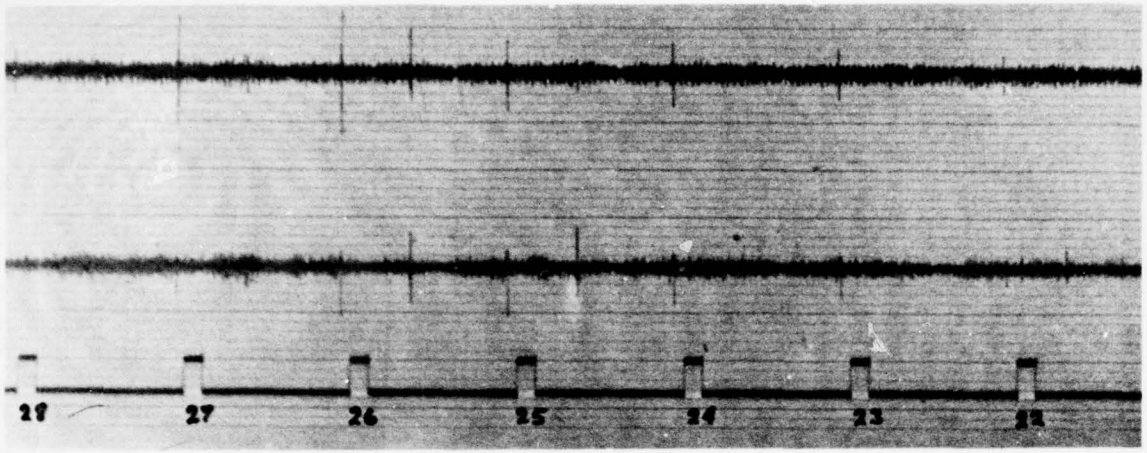

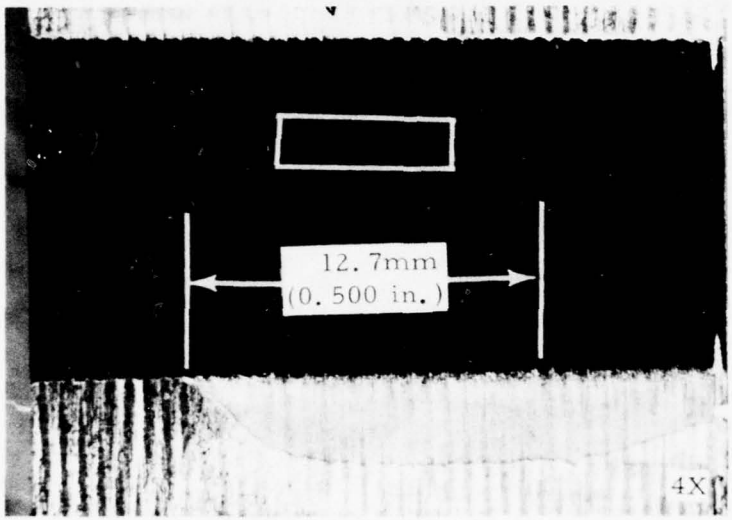

FIGURE 22. MAGNETIC SIGNATURE AND SECTIONING RESULTS - SPECIMEN NO. 30, LOT 2-12

signatures. The other signature location investigated on Specimen No. 30 was in the Ogive region between 8.9 and 9.8-in. from the start of the exterior inspection run. Inspection records from the two side-by-side coils and a photograph of the metallurgical sectioning results are shown in Figure 23. The stringer-type inclusion was approximately 0.006-in. below the exterior surface and the exposed length extends approximately 0.55-in. in the axial direction.

Two signature locations from Specimen No. 10 were investigated. One of these was in the Ogive region, between 16.0 and 16.9-in. from the start of the exterior inspection run. Figure 24 shows the inspection records with very prominent signatures along with a photograph obtained during the metallurgical sectioning sequence. The sectioning investigation disclosed a long, stringer-type inclusion which extends for approximately 1.0-in. along the axial direction and ranges from approximately 0.020-in. to approximately 0.06-in. below the exterior surface. Dashed lines in the illustration indicate the extent of the inclusion. Specimen 10 was also investigated at an axial flux parallel (X) component signature location in the Bourellet section between 3.6 and 4.1-in. from the start of the exterior inspection run. Records from the four probe coils (1 channel of the Visicorder galvenometers was not functioning) along with a photograph (edge view, etched) obtained during the metallurgical sectioning sequence are presented in Figure 25. The metallurgical investigation disclosed a stringer-type inclusion which extends for approximately 1-in. in the axial direction and approximately 0.015-in. wide (circumferentially) by 0.006-in. thick (radially), extending approximately parallel to the surface and located approximately 0.012-in. below the exterior surface.

Specimen No. 3 was metallurgically investigated at three signature locations obtained during an interior circumferential flux orientation normal (Y) component scan. The records in Figure 26 and 27 show several prominent signatures marked A, B, C, D, E, and F that are located in the Ogive region between 14.3 and 15.7-in. from the start of the magnetic inspection run.

Cracks associated with signatures A, B and C are shown in the metallurgical sectioning views. Crack A was approximately 0.015-in. deep and extended through one edge of cylindrical specimen. Crack B was approximately 0.045-in. deep and extended through both edges of the cylindrical section. Analysis of the records indicates that it extends for approximately 1-in. beyond the section toward the Bourellet region and also extends into the Ogive region. Crack C is approximately 0.025-in. deep and also extends beyond each edge of the cylindrical section.

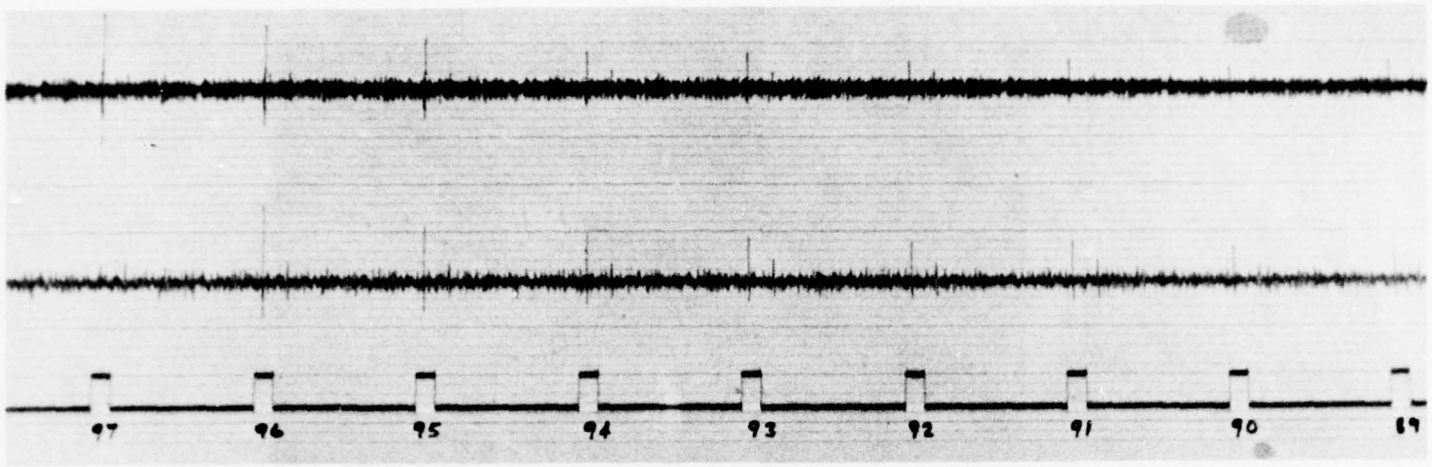

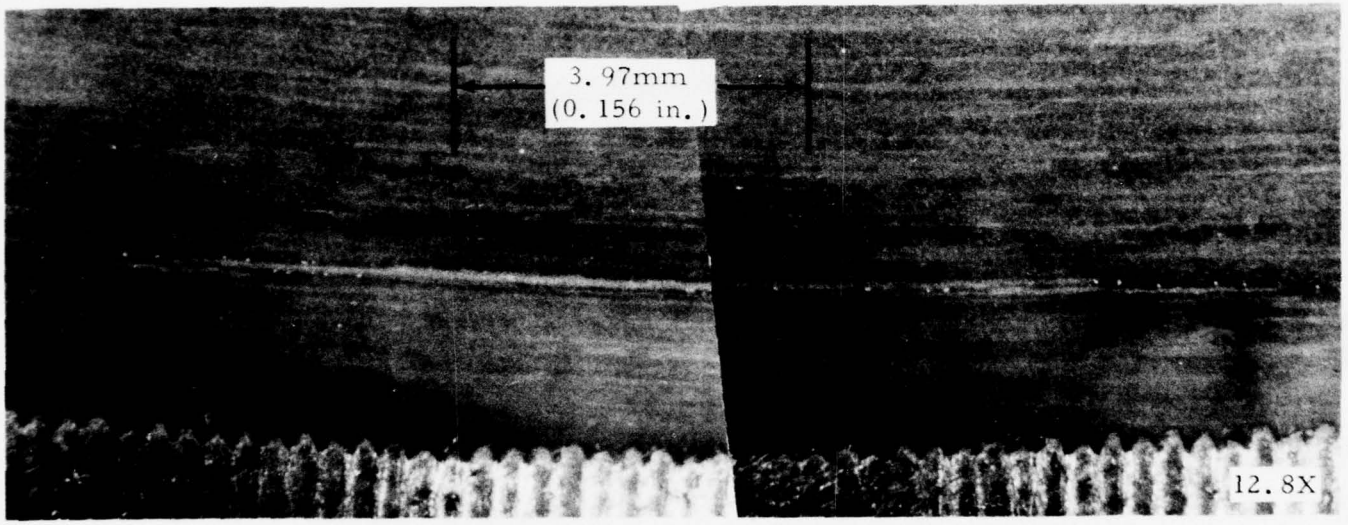

FIGURE 23. MAGNETIC SIGNATURE AND SECTIONING RESULTS - SPECIMEN NO. 30, LOT 2-12

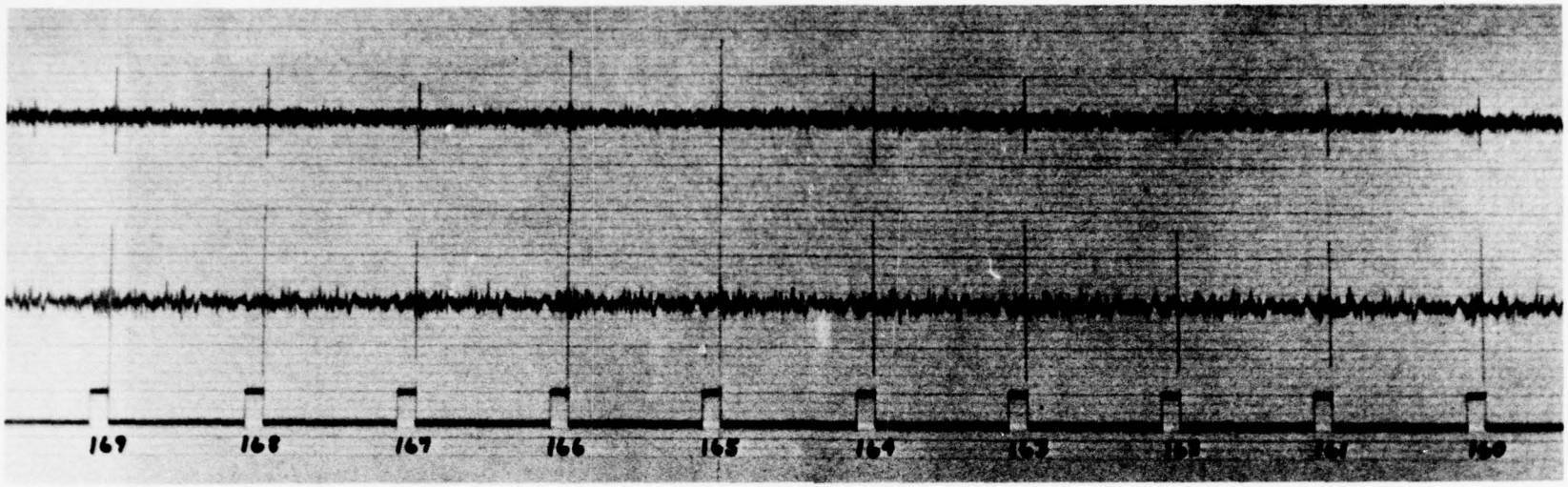

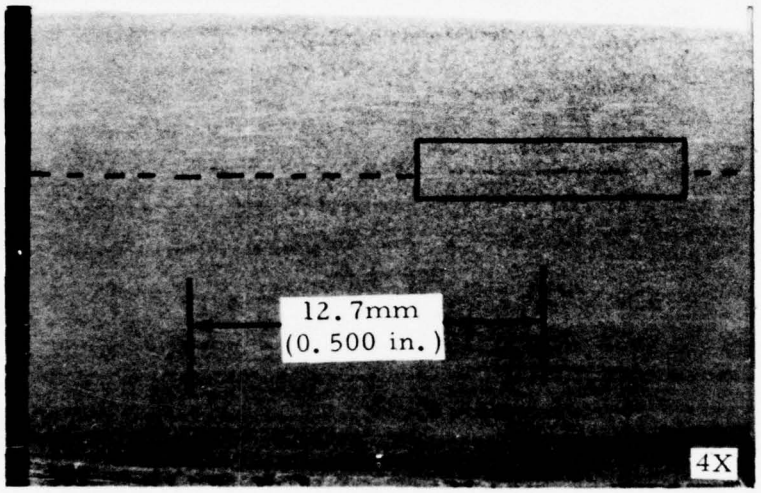

FIGURE 24. MAGNETIC SIGNATURE AND SECTIONING RESULTS - SPECIMEN NO. 10, LOT 2-12

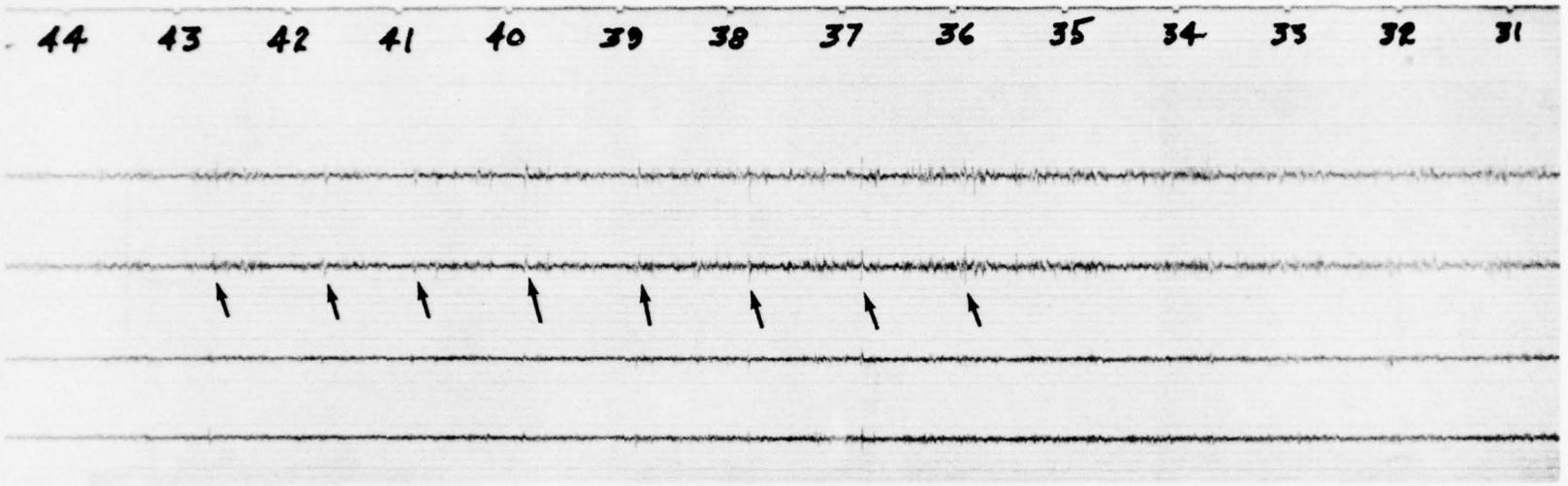

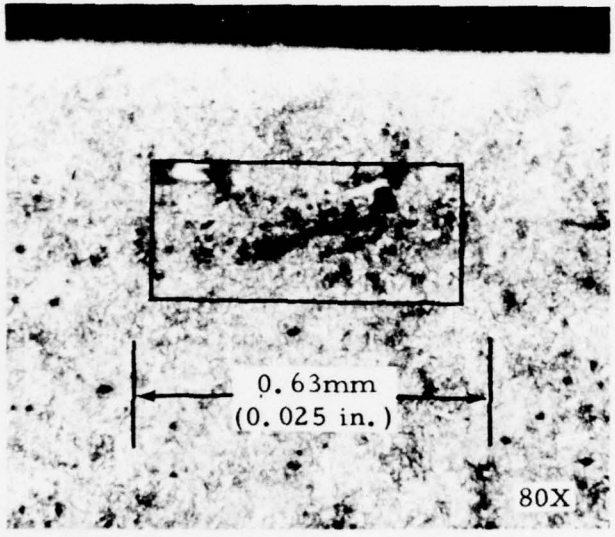

FIGURE 25. AXIAL TRACE, SECTIONING RESULTS - SPECIMEN NO. 10, LOT 2-12

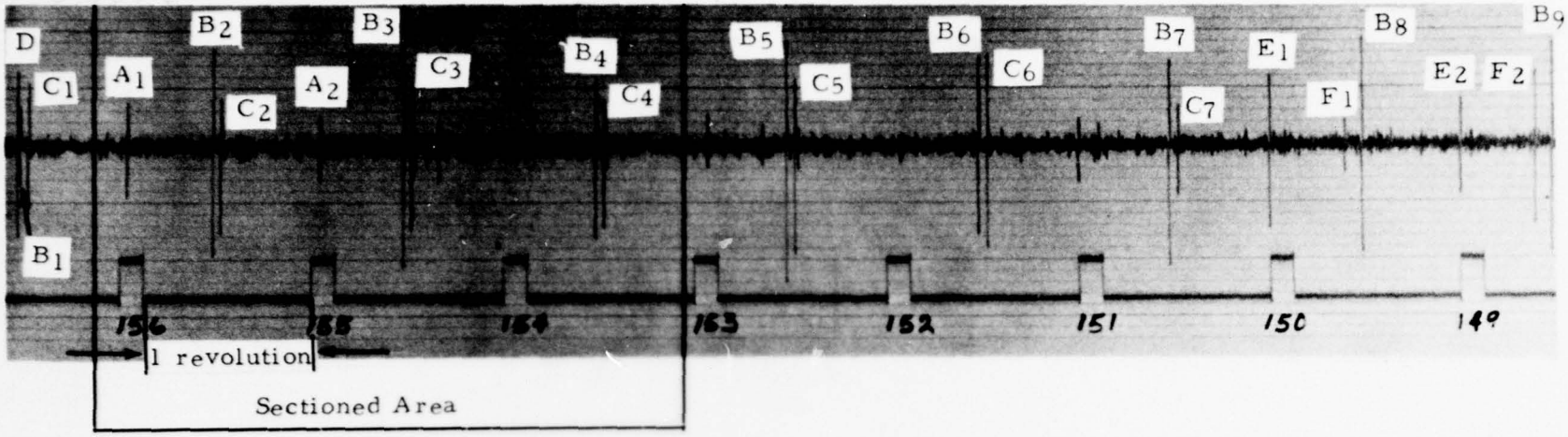

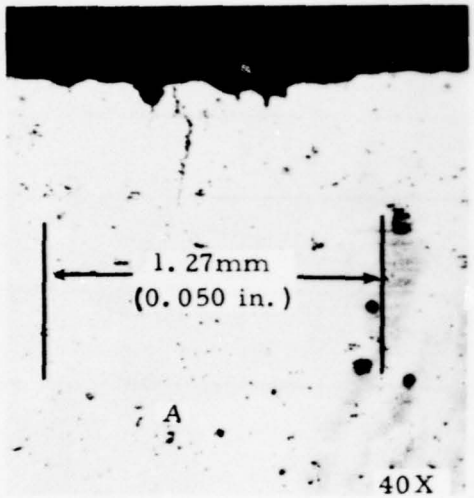

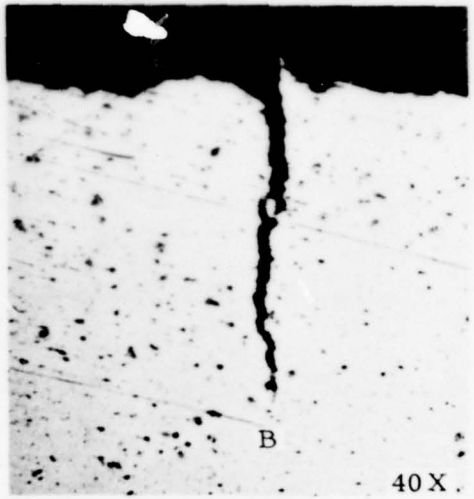

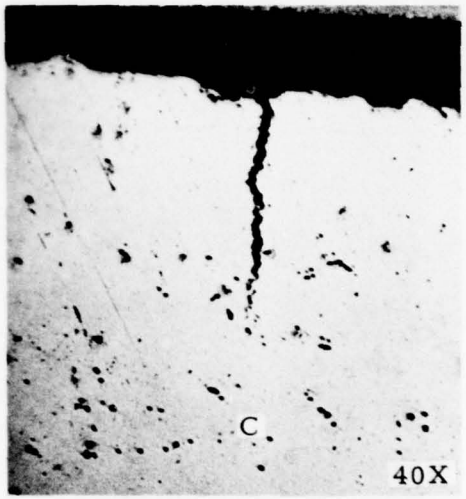

FIGURE 26. MAGNETIC PERTURBATION INSPECTION RECORD WITH PHOTOGRAPHS OF SEVERAL SIGNATURES AND ASSOCIATED CRACKS CONFIRMED BY METALLURGICAL SECTIONING (Specimen 3, Lot 2-12)

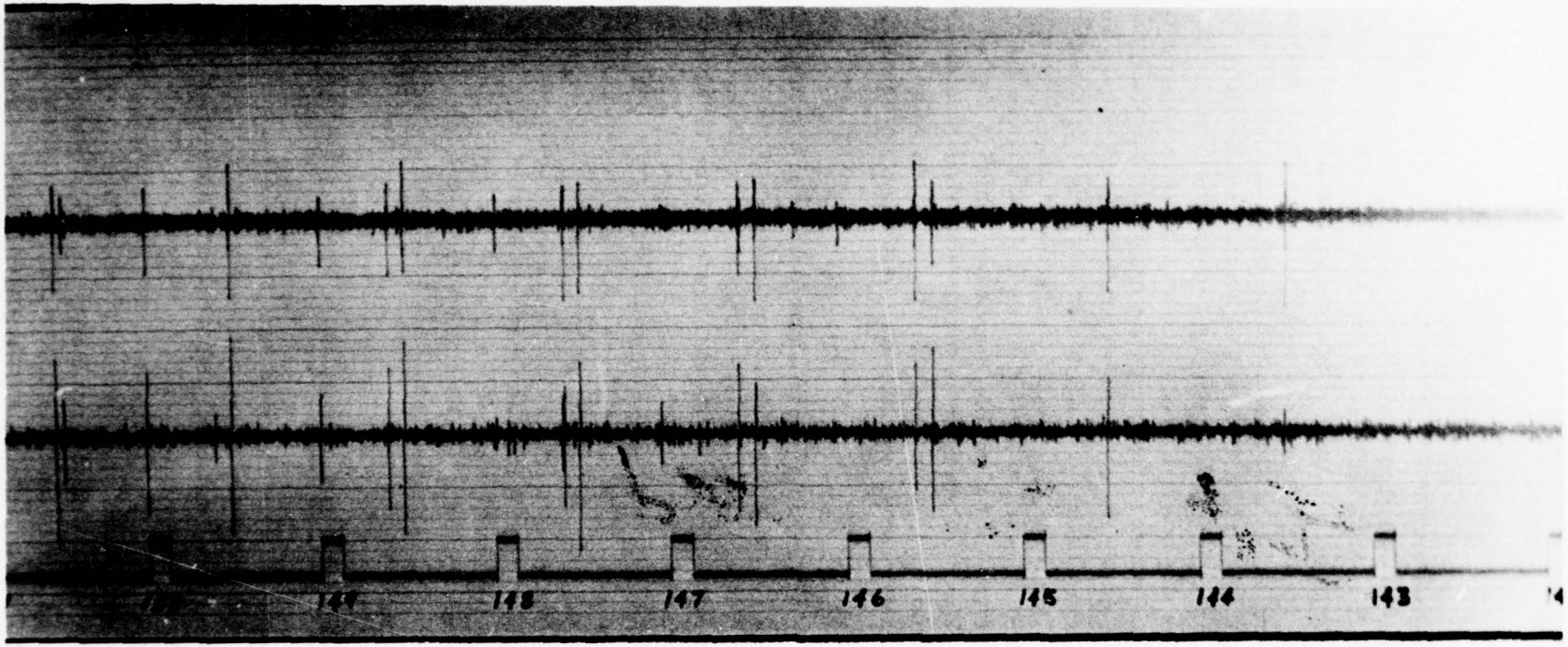

FIGURE 27. CONTINUATION OF MAGNETIC RECORD OF FIGURE 26

The Ogive end of Specimen No. 3 was also investigated using the magnetic particle inspection method. A photograph of the indications is shown in Figure 28. Several cracks are indicated and detailed analysis of the magnetic inspection records, Figures 26 and 27, and the magnetic particle indications confirmed precise spatial correlation between several of the cracks and the signatures indicated by corresponding letters (D, A, C, B) in Figures 26, 27 and 28. Magnetic particle indication B is rather faint in the photograph, however when viewed with low magnification under a stereo microscope the indication and the crack were apparent. While it is rather easy to detect cracks using the magnetic particle method applied to this Ogive region cut from a complete projectile, it should be obvious that detection of these cracks by a magnetic particle examination of the complete projectile would be somewhat more difficult. By contrast, the magnetic perturbation signatures of Figures 26 and 27 are so prominent that automatic detection using simple signature analysis equipment would be very reliable. In fact, detection of smaller cracks would also be possible. Furthermore, it would not only be possible to detect the crack, but also to determine the approximate size using computer-assisted signature analysis procedures.

During visual inspection examination of the interior surfaces of the projectiles, a large depression-type flaw was observed on the interior surface of Specimen No. 37 in the Ogive region. Since this was such a large flaw, it was anticipated that signatures could be obtained on an exterior scan over this interior flaw region. Figure 29 shows the two records obtained from the side-by-side coils during an external circumferential flux inspection. The signatures are very prominent and extend for approximately 1.3-in. Also, the shape is somewhat unusual, indicating that the flaw is not symmetric. Furthermore, the peak separation is more pronounced than was the case for the previous sectioning results and this is anticipated since the flaw is approximately 5/16-in. beneath the surface inspected. The silicon rubber replica of the flaw indicates approximate correspondence between the total length of the flaw and the region over which signatures are obtained.

D. Signal Analysis and Imaging

Because of the extensive equipment design and fabrication required to adapt existing hardware to accommodate both circumferential and axial magnetization with inside and outside scans, plus fixture for limited investigations of the exterior base region, it was possible to allocate only limited funds for signature analysis and imaging investigations. Nevertheless, results which are extremely encouraging were achieved and will be reviewed briefly. As indicated earlier, data were recorded on analog magnetic tape during inspections of each projectile. Records from selected specimens were used for signal analysis and imaging investigations.

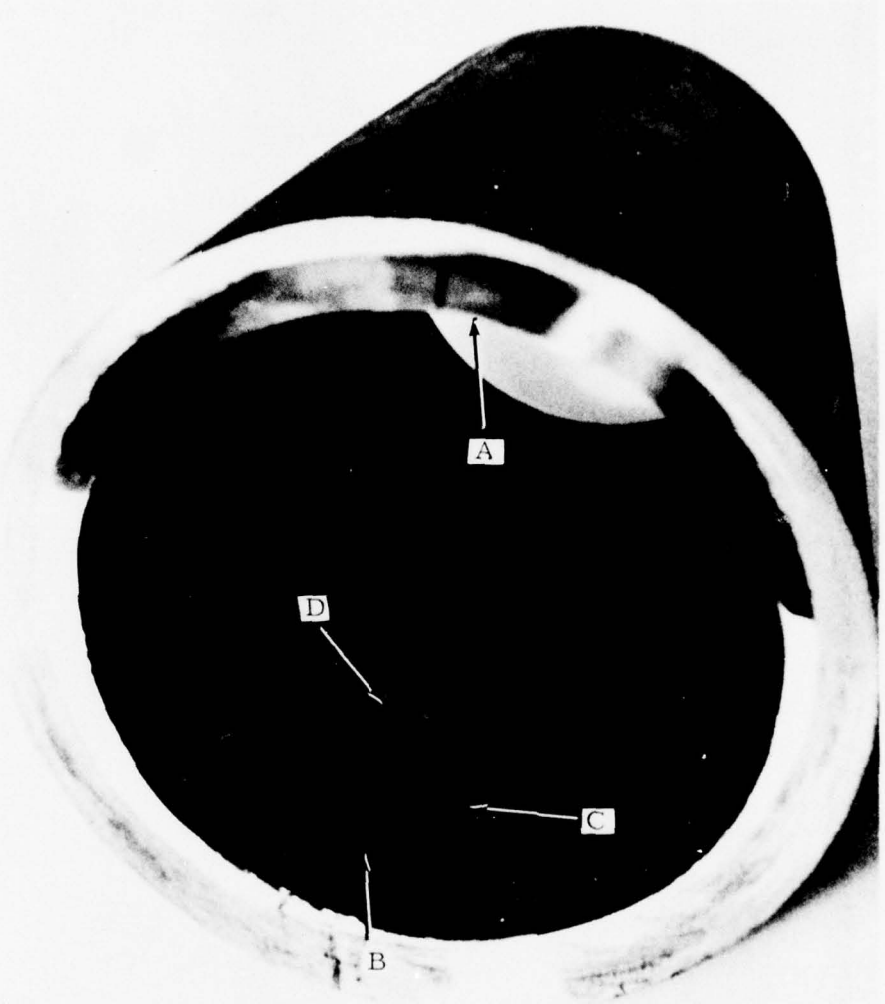

4465

FIGURE 28. MAGNETIC PARTICLE INDICATIONS ON OGIVE SECTION OF SPECIMEN NO. 3 (A, B, C, and D correspond precisely with signatures A, B, C, and D of Figures 26 and 27)

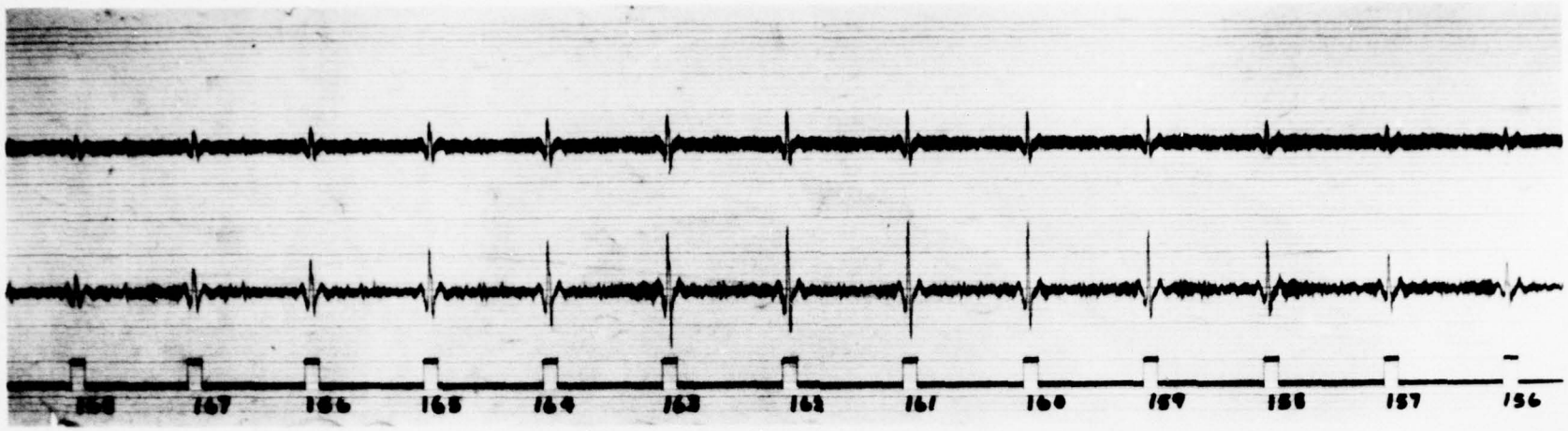

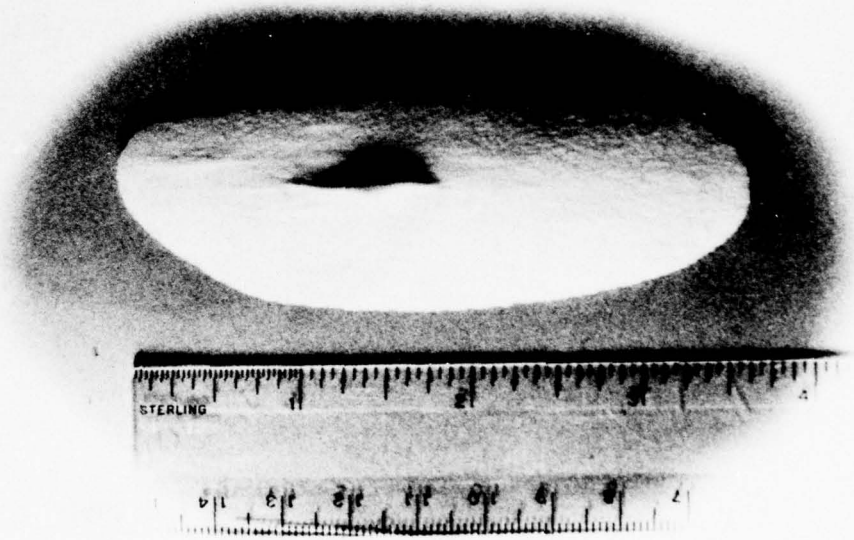

FIGURE 29. MAGNETIC SIGNATURE AND REPLICA OF INTERNAL DEFECT - SPECIMEN NO. 37, LOT 2-14

The images were developed by use of a black-and-white television monitor in combination with an image-memory-scan converter. This instrumentation system, known as "Lithicon", forms the basis for an image storage system in which values of an applied intensity signal can be directly stored in an X-Y matrix. The process is similar to the conversion of a visual image to a charge pattern in a television camera tube (Vidicon). Since the Lithicon is not a direct viewing tube, the stored charge pattern in "read out" by addressing locations on the target with an electron beam and using the generated signal as an input to a television monitor. By appropriate control of the beam the device can store amplitude signal variations in intensity or grey-scale variation, with a quality equivalent to high-resolution black-and-white photography. Once stored, the image can be retained for long period of time (hours to weeks) and the intensity variations can be nondestructively read out repeatedly for image construction.

For these investigations the records from one probe coil which sensed the normal (Y) component of circumferentially oriented flux was acquired during a circumferential scan. Figure 16, page 23, illustrates the sequence and the Visicorder record shows the conventional presentation of time-serial data acquired as a probe is scanned over the target flaws in the reference specimen. Figure 30 shows the more effective presentation of these data as a direct image using a C-scan format. In this format, the display-device beam position represents the probe location on the surface of the projectile and signal amplitude variations from the probe are represented by a grey-scale variation ranging from black (maximum amplitude) to white (minimum amplitude). An image of the complete projectile inspection is shown and consists of 154 scans at 0.1-in. spacing. Both simulated and actual flaws are shown in this image as dark areas. The simulated flaws are indicated in Figure 30a by the outline and Figure 30b shows an expanded area to display these flaws more clearly. For comparison, a schematic of the target flaws is also shown. Missing flaws on the image are a result of the flaw orientation relative to the applied magnetic field direction, flaw size, sensor probe resolution and signal analysis parameters. While only signals from one of the two probes in the magnetic perturbation sensor array were used to develop the images shown in Figure 30, circuitry was breadboarded to give an image developed from the combination of both probes; however, a failure in the reproduce electronics of the tape recorder prevented display of combined images. Even though the illustration shows only half of the resolution possible in the displayed image, the result in the C-scan format is obviously an effective display of inspection results.

A similar image display obtained from the magnetic recordings acquired during inspection of Specimen No. 3 along with the magnetic particle indications of this specimen are shown in Figure 31. The excellent correspondence between cracks B, C, and D is apparent.

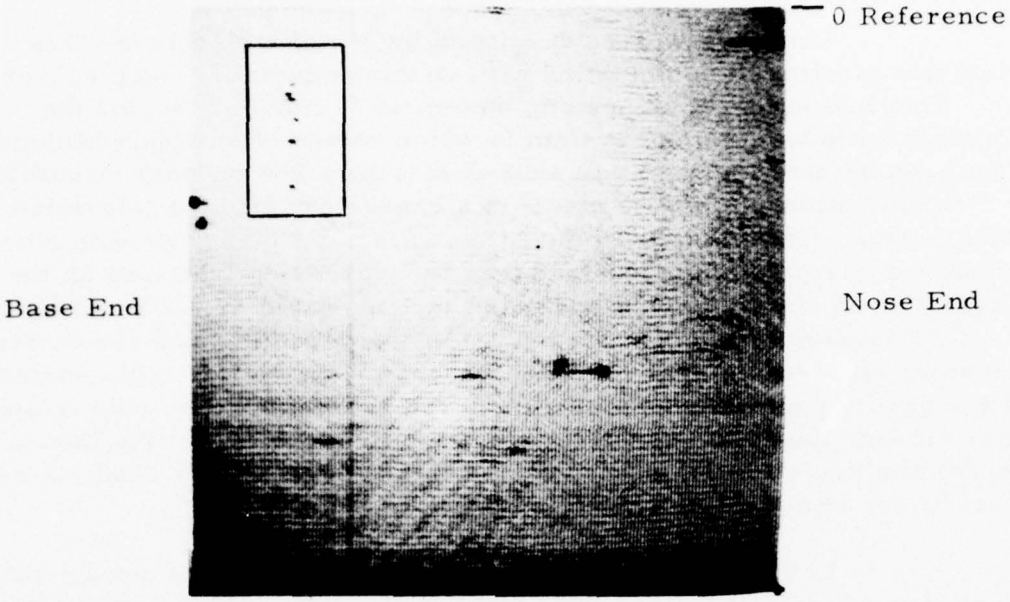

a. Direct Image - Full Scan of Projectile Casing Interior with Circumferential Magnetization

4362a

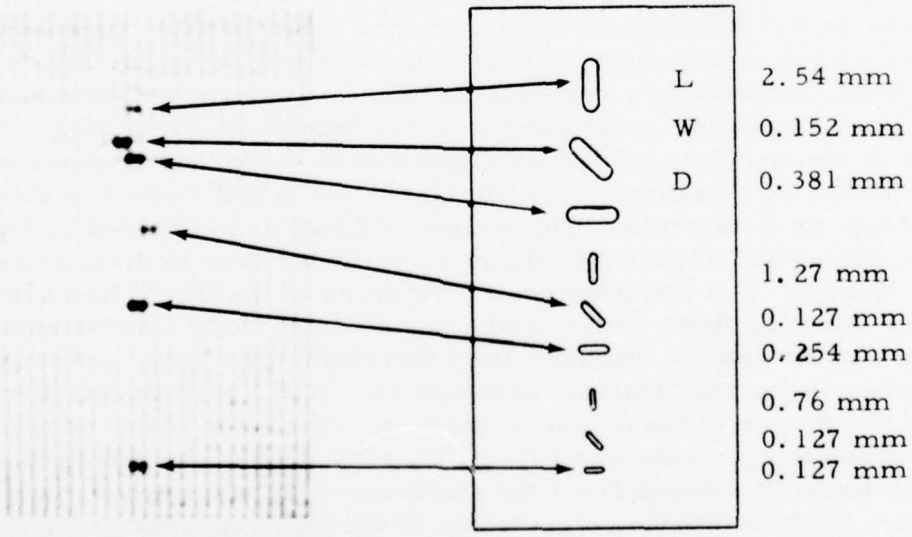

b. Expanded Image of Simulated Flaws

c. Defect Schedule of Simulated Flaws

FIGURE 30. DIRECT IMAGING OF A MAGNETIC FIELD PERTURBATION INSPECTION

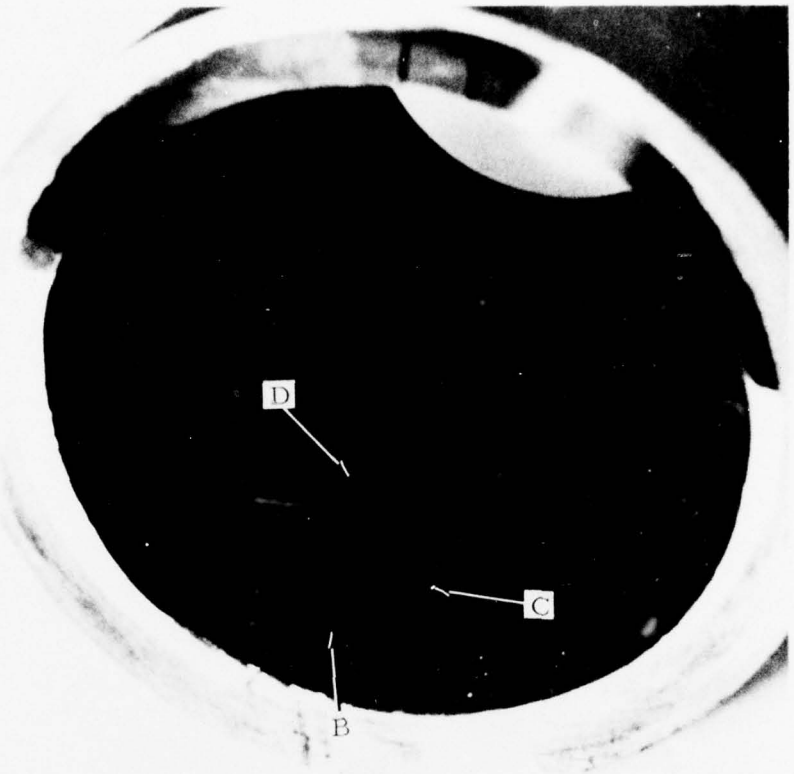

4466

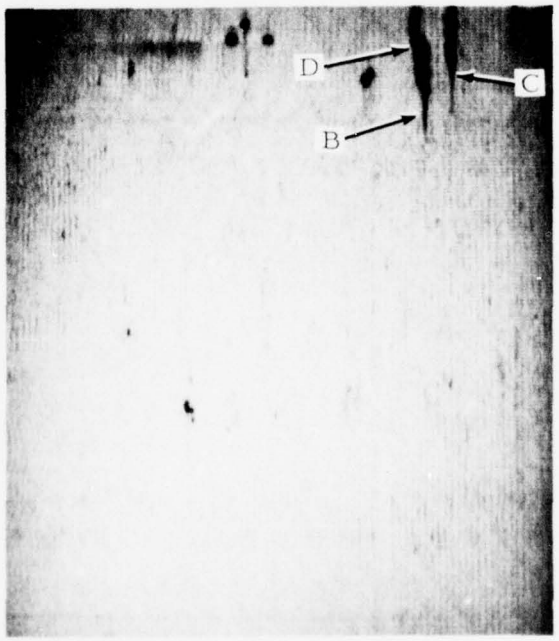

FIGURE 31. EXAMPLE OF IMAGE DERIVED FROM MAGNETIC PERTURBATION RECORDS ILLUSTRATING CORRESPONDENCE WITH CRACKS

As indicated earlier, only a limited signal analysis and imaging display investigation was possible. However, with additional effort it would be possible to image flaws in their respective locations in a plan dimension as well as through the thickness to indicate approximate location in the projectile wall. In addition, by setting different threshold levels it would be possible to select the minimum size flaw desirable for display. Although considerable effort will be required it would also be possible to reconstruct a three-dimensional image of the magnetic signatures thereby providing a basis for readily differentiating between cracks and stringer-type inclusions based upon the characteristic shapes associated with these two different type flaws.

V. DISCUSSION

Considerable design, fabrication, assembly and operational checkout was required of elements to permit adaptation of existing equipment for circumferential and axial inspection of the body and circumferential inspection of the base of the 155mm projectile. The bench-type apparatus performed satisfactorily at rotational speeds of approximately 190 rpm and axial traverse of 19-in. /min.

Signatures obtained from the target flaws machined in the reference specimen indicated excellent sensitivity with circumferential flux orientation for flaws with the major dimension oriented, axially, along the projectile axis. For flaws with an orientation at 45° to this axis, the signature amplitude is reduced by a factor of approximately 4 and the peak separations are exaggerated. Even for flaws oriented at 90° to this axial direction signatures are still obtained provided the flaw has significant cross-sectional area normal to the flux; for such circumferentially extended flaws, the amplitude is reduced by a factor of approximately 10 and again, the peak separations are markedly exaggerated. For a greatly extended flaw oriented at 90°, signals would be obtained only at the two ends. It was possible to produce a relatively high flux density with the magnetic circuit arrangement designed for circumferentially oriented flux. Accordingly, signature amplitudes from target flaws were large enough that electronic system noise was not a factor in determining signal-to-noise ratio and only the reproducible magnetic background signatures from the projectile was considered the limiting noise factor.

For flaws with the major dimension in the circumferential direction, the analysis indicates that flux oriented along the axial direction would produce the best signal-to-noise ratio. Results from the target flaws in the reference specimen confirmed these analyses. However, the signature amplitude obtained from the target flaws was significantly less than in the case for the circumferentially oriented flux. The primary reason for this was the fact that even though a large magnetizing coil was used, which produced 525 oersteds on the coil axis, the short length of the projectile compared to the cross-sectional area resulted in a large demagnetizing factor at the ends of the projectile. Flux density in the projectile wall could be increased by using a magnetic yoke oriented along the projectile axis to concentrate the flux in this region. However, as the ends of the projectile are approached the flux density would decrease drastically and the orientation of the flux would also change. Use of magnetic cylinders with an axis along the axis of the projectile at either end of the projectile could be used to extend the magnetic circuit thereby decreasing the demagnetizing factor and increasing the flux density.

During the investigations on this program where axial magnetization was used, the projectile was magnetically lengthened by using an iron cylinder, 3-in. in diameter with a 0.75-in. wall and 12-in. long (see Figure 13). For the base end of the projectile the rocket motor body was utilized to extend the magnetic flux path (see Figures 11 and 12). If investigations and/or analyses have indicated that circumferentially oriented flaws are a problem then axial flux magnetization should be incorporated in prototype and production equipment. No signatures indicative of significant flaws oriented in the circumferential direction were obtained during the investigations conducted on this program.

The experimental arrangement for inspecting the base region on the outside surface as shown in Figure 14 was intended to examine this region using a spiral scan as the probe is advanced from the outer periphery near one pole piece toward the center of the projectile. Because of a large magnetic gradient encountered by the probe as the base was scanned from one pole piece toward the other, signatures from test flaws could not be resolved with this probing arrangement. It is reasonable to anticipate that flaws oriented in the axial and/or radial direction of the base could readily be resolved by an arrangement producing circumferential flux and by locating the probe at a fixed location mid-way between the two pole pieces. A scan of this region could be obtained by rotating the projectile and slowly advancing the probe toward the center of the base. It is anticipated that the gradient change would not be nearly as rapid and, as long as the scan speed is relatively low it would be possible to electronically filter the gradient signal and pass the higher frequency component associated with flaw signatures. It was not possible within the funding available to conduct such experiment; however, this arrangement is similar to an arrangement used successfully on a previous program for the examination of thrust washers of a propeller blade assembly. No probing arrangement was attempted for the interior base region; however, with modifications the internal probe could be used to examine more of the radius section than was actually accomplished during this investigation.

No attempt was made to examine the thread relief region at the base of the projectile and examination of this region would have been impossible with the base holding fixture that was used for the investigations on this program. With a suitable design it would be possible to examine this region for inclusions, cracks, and other type flaws. Since this has been indicated as one of the critical region in Ref. 1, it may be appropriate to consider incorporation of this inspection in prototype designs.

An overall appraisal of results obtained on this program in conjunction with extensive results obtained on other programs during experimental investigations, equipment designs, and extended operational service

provide a strong foundation for proceeding with equipment design. Specific equipment examples include magnetic perturbation equipment for CH46 rotor blade spar inspection (Ref. 2) which has been in service at overhaul depots since 1967. A more recent example incorporating more advanced electronic logic for signature analysis is the CIBLE equipment (Ref. 3) designed for inspecting ball and roller bearing components; systems have been delivered to the Army, installed at CCAD, and to the Air Force, installed at Tinker AFB. Essentially no new technology is required to accommodate the method to the routine high-speed inspection of artillery projectiles.

The signature analysis and imaging investigations were very encouraging and with a more comprehensive effort could provide the electronic logic and associated elements for analyzing signatures, categorizing results, and assessing these results against an accept/reject criteria and automatically categorizing projectiles as acceptable, reject, and questionable or possibly rework. The image display methods could provide a video display of the results which could be photographed to provide a time-serial record of each projectile inspected and could also provide a compact, high-density information, permanent record on microfilm. The video display could also be effective in maintaining operator interest, provide a method of supervisory checks, would be useful for training purposes and also for displays.

Most inspections were obtained at a rotational speed of approximately 190 rpm. With suitably designed equipment it is reasonable to anticipate that rotational speeds as high as approximately 400 rpm could be satisfactorily achieved. Time to inspect a projectile is a combination of probe size (width of inspection track per probe), helix angle, rotational speed, and projectile surface length. Assuming two probe channels each on the exterior and interior surfaces for simultaneously measuring the circumferential component normal to the projectile surface, a probe advance of approximately 0.1-in. per revolution and a rotational speed of 200 rpm, the interior and exterior surfaces could be inspected in approximately 0.9 minutes (54 seconds). From these calculations it is apparent that a relatively high-speed inspection can be accomplished.

VI. CONCEPTUAL DESIGN

A preliminary conceptual design of an inspection system for the artillery projectile incorporating the magnetic perturbation method is shown in the sketch of Figure 32. Briefly, the system consists of elements to accommodate simultaneous inspection of the interior and exterior Bourellet and Ogive surfaces of two projectiles. Inspection would be accomplished with the projectiles oriented vertically and rotated by chucks clamping the base. Circumferential magnetization would be provided by a single magnetic circuit with four pole pieces. This arrangement would result in balanced magnetic forces on the machine, minimize the inspection time, and offer other advantages with only slight increase in complexity.

The base of this equipment would contain a drive mechanism for projectile rotation, rapid traverse mechanism for probe positioning and retraction, gearing for predictable scanning motion, shaft position encoder and safety interlocks. The two lead screw columns provide support and traverse capabilities to the magnetic circuit and interior and exterior probe mechanisms. The projectile shaped cam would mechanically control pole piece location as the vertical traverse is made. Alternatively, numerically controlled drives for the pole pieces could be incorporated; this approach, while initially more expensive, would simplify changeover to other projectile configurations. The electronic console, in the background, contains the video display, tape recorder, electronic signal analysis and logic circuits, and the necessary functional controls.

It should be pointed out that it has been assumed in the foregoing that an operator interface has been provided. We believe this to be necessary, at least during the early stages of use, in order to develop confidence in the procedure and to aid in developing a statistical base for accept/reject criteria, which at a later date could eliminate the need for operator interpretation and control.

A description of a typical operational sequence follows. The projectile would be loaded into the inspection station, either manually, by crane, or perhaps automatically in a vertical position. During this loading operation the probe assemblies would be withdrawn to a protected position. The operator, in a control and instrumentation booth, would then actuate the "start inspection" sequence. This would clamp the projectile, advance the probes to the inspection position, control the magnetizing circuit, initiate the scanning mechanism, retract the probes after completion of scan and shut the system down, ready for reloading. During the inspection scan the operator would have displayed, in real-time, the results of the inspection on a video display device. Signal analysis equipment coupled

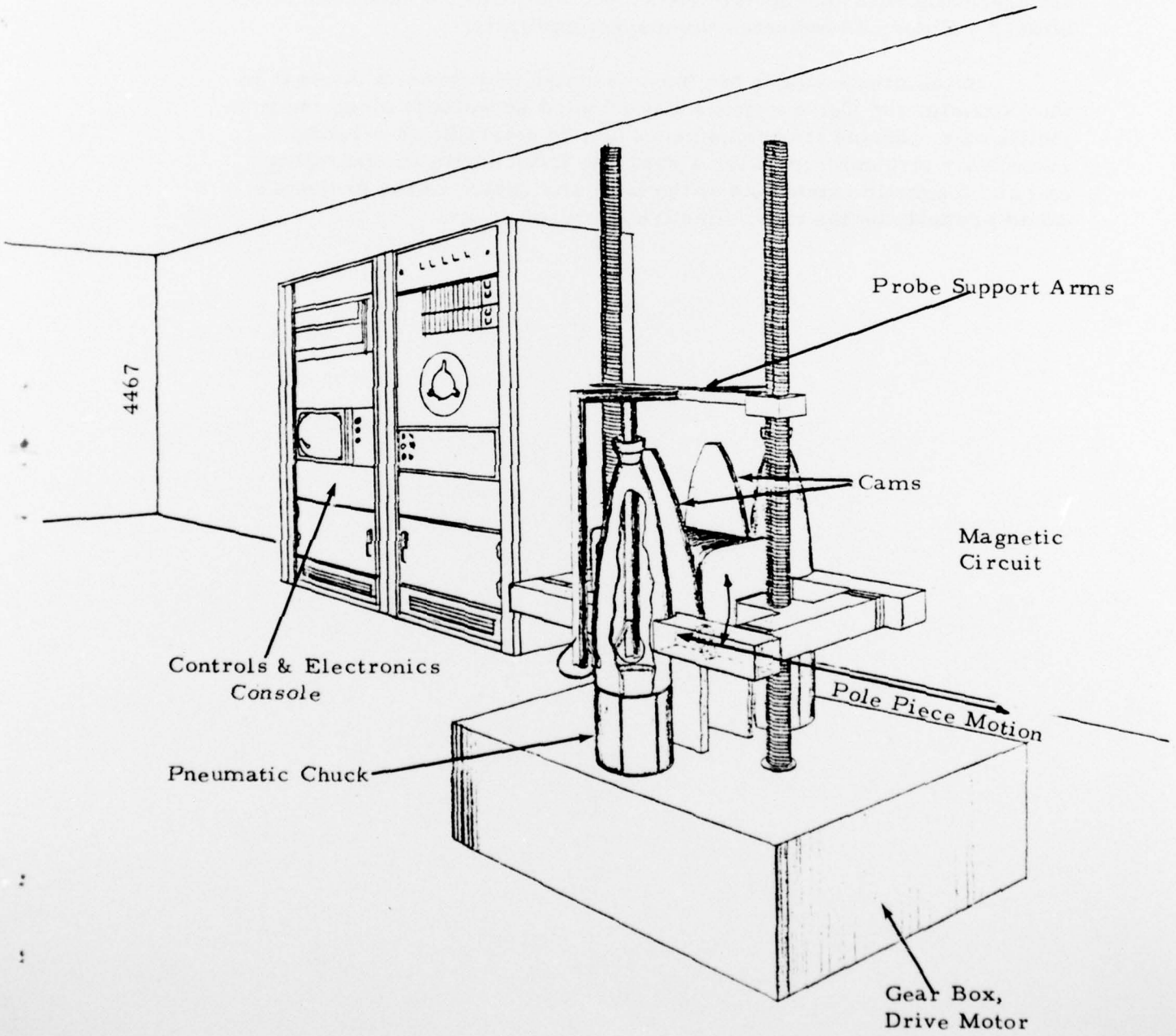

FIGURE 32. CONCEPTUAL INSPECTION DEVICE FOR PROJECTILES

to the display device would have been pre-set to display only significant defect signatures. If no defect signatures occur, the operator presses the accept button. If defect signatures occur, upon pressing the reject button the information would be transferred to magnetic tape from the display device memory for further study and the inspection head reset for the next inspection. The accept/reject criteria could be applied automatically with appropriate electronic logic after a data base is established. Figure 33 indicates the inspection limits.

In the preceeding it has been assumed that flaws of interest in the Bourellet and Ogive regions are oriented essentially along the projectile axis. Should it become necessary to detect flaws oriented essentially circumferentially, a separate fixture with an encircling coil and magnetic extensions at the base and "nose" of the projectile would probably be the most effective approach.

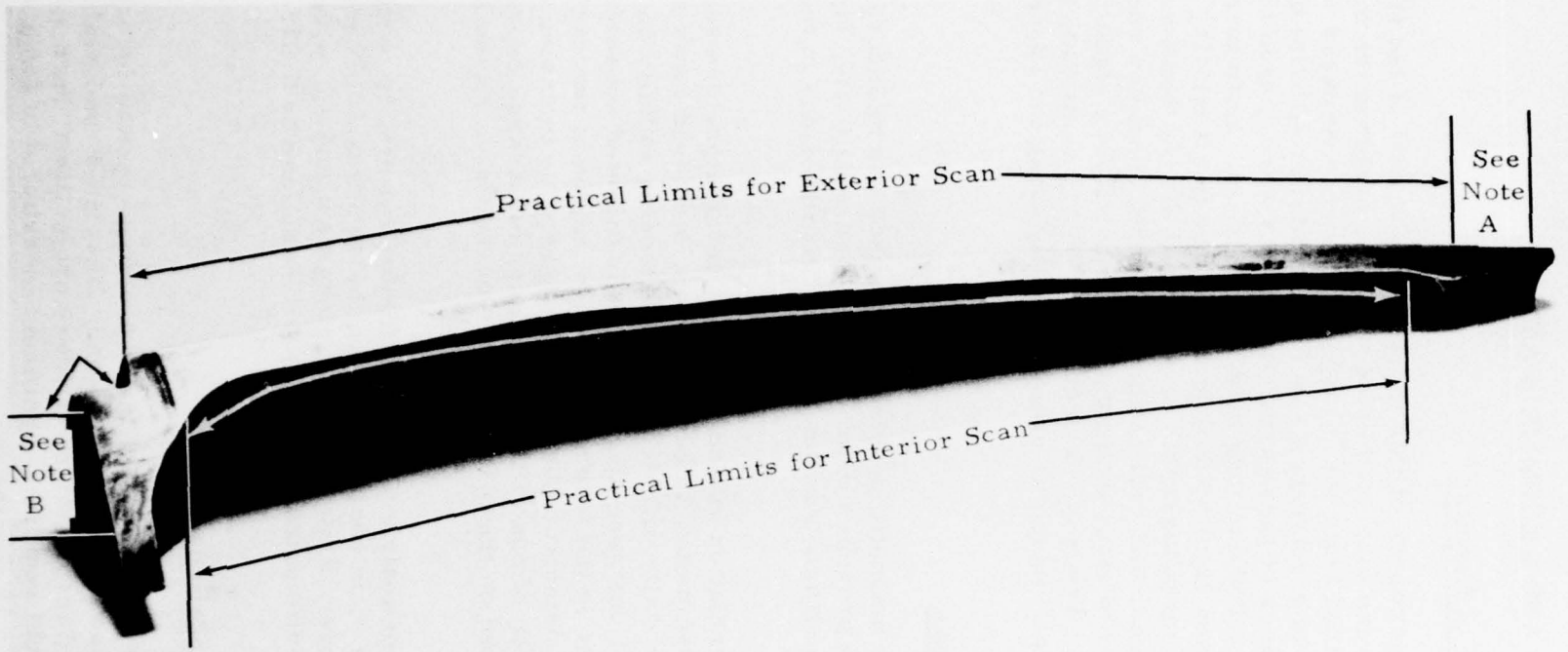

Notes: A. Area is accessible for inspection; however, anomalous signals would be caused by stamped identification markings.

B. These areas of the projectile are accessible; however, a separate fixture would be required.

FIGURE 33. PRACTICAL SCAN LIMITS FOR CONCEPTUAL DESIGN

VII. CONCLUSIONS AND RECOMMENDATIONS

A. Summary of Results

During the course of this investigation a total of ten (10) specimen projectiles were inspected using magnetic perturbation methods. Defect signatures obtained from these inspections were compared with signatures obtained from a reference specimen in which artificial defects had been machined. Sizes of these artificial defects were chosen to bracket the target flaw size of 0.050-in. long by 0.015-in. deep. Examination of inspection results showed significant flaw signatures in all ten (10) specimens examined. Subsequent metallographic sectioning at six (6) locations on three separate specimens, and replication on a fourth specimen showed excellent correlation as to size, location, and extent of flaw signatures from these specimens. Types of flaws observed during sectioning were cracks and stringer-type inclusions oriented axially along the specimens examined.

B. Conclusions

1. The magnetic perturbation method can be incorporated into equipment that can provide a reproducible, high sensitivity, high-speed, automatic nondestructive inspection of critical regions in the artillery projectile.

2. Correlation investigations of seven signature sequences from four individual specimens, in each instance, disclosed flaws of target size or greater; three axially oriented cracks extending radially on the interior Ogive region of one specimen; two axially oriented subsurface stringer-type inclusions on the exterior Bourellet region of two of the specimens; one axially oriented subsurface stringer-type inclusion on the exterior Ogive region of one of the specimens; and a large depression-type flaw axially oriented on the inside surface of the Ogive region in the fourth specimen.

3. From analyses of the sectioning results, in particular Location A of Specimen 3, in conjunction with the significant S/N ratio of the signature from "target" Flaw 1 (0.03-in. long by 0.005-in. wide by 0.005-in. deep), it is anticipated that a flaw 0.05-in. long by 0.015-in. deep can be detected.

C. Recommendations

1. It is recommended that a prototype system incorporating the magnetic perturbation method be designed, fabricated, and evaluated for performing a high-speed inspection of artillery projectiles. Such specially designed equipment would require a significant investment of funds and would require a period of 12 to 18 months for development.

2. After operational checkout a large number of projectiles should be inspected and comprehensive analyses and correlation investigations conducted to establish a quantitative basis for an "accept/reject/other" disposition criteria.

REFERENCES

1. Hartman, H., "Ultrasonic Inspection of High Fragmentation Warheads for 155mm HE RAP Cartridge M549", Tech. Rept. 4968, Nov. 1976, Picatinny Arsenal, Dover, NJ, Braun, M.F., Appendix C to Rept. 4968, "Destructive Analysis of Ultrasonically Rejected Warheads, 155mm RAP M549, Mason & Hanger - Silas Mason Co., Inc., Iowa Army Ammunition Plant, Engineering Dept., Burlington, Iowa 52601.

2. Birdwell, J.A., Kusenberger, F.N., Barton, J.R., "Development of Magnetic Perturbation Inspection System (A02GS005-1) for CH-46 Rotor Blades", Technical Summary Report, SwRI Project No. 15-2189, 11 Oct. 1968.

3. Barton, J.R., Kusenberger, F.N., Hampton, P.L., Bull, H., "Critical Inspection of Bearings for Life Extension (CIBLE)." Proc. of 10th Symposium on NDE, April 23-25, 1975, San Antonio, Texas.

DISTRIBUTION LIST

No. of Copies	To
1	Office of the Director, Defense Research and Engineering, The Pentagon, Washington, D. C. 20301
12	Commander, Defense Documentation Center, Cameron Station, Alexandria, Virginia 22314
1	Advanced Research Projects Agency, The Pentagon, Washington, D. C. 20315
	Metals and Ceramics Information Center, Battelle Columbus Laboratories, 505 King Avenue, Columbus, Ohio 43201
2	ATTN: Mr. Daniel Maykuth
	Chief of Research and Development, Department of the Army, Washington, D. C. 20310
2	ATTN: Physical and Engineering Sciences Division
1	Dr. Bernard R. Stein
	Commander, U. S. Army Materiel Development and Readiness Command, 5001 Eisenhower Avenue, Alexandria, Virginia 22333
1	ATTN: DRCDE-DE, Development Division
1	DRCDE-RS, Research Division
1	DRCDE-RS, Scientific Deputy
1	DRCLDC, Mr. R. Zentner
	Commander, U. S. Army Aviation Research and Development Command, P. O. Box 209, Main Office, St. Louis, Missouri 63166
1	ATTN: DRSAV-LEP, Mr. J. M. Thorp
1	DRSAV-ER, Dr. I. Peterson
	Commander, U. S. Army Missile Research and Development Command, Redstone Arsenal, Alabama 35809
1	ATTN: DRSMI-IE, Mr. J. E. Kirshtein
1	DRSMI-R, Mr. John L. McDaniel
1	DRSMI-RBLD, Redstone Scientific Information Center
1	Chief Scientist, Dr. W. W. Carter
1	Directorate of R&D
1	Dr. B. Steverding
	Commander, U. S. Army Mobility Equipment Research and Development Command, 4300 Goodfellow Boulevard, St. Louis, Missouri 63120
1	ATTN: DRSME-PLC, Mr. J. Murphy
1	Commander, U. S. Army Tank-Automotive Research & Development Command, Warren, Michigan 48090
1	ATTN: DRDTA-PPS, Mr. David Siegel
1	Mr. B. A. Schevo

No. of Copies	To
	Commander, U. S. Army Armament Materiel Readiness Command, Rock Island, Illinois 61201
2	ATTN: DRSAR-QA
1	DRSAR-QAE
	Commander, U. S. Army Armament Research and Development Command, Dover, New Jersey 07801
1	ATTN: DRDAR-SCM, Dr. K. Iyer
1	DRDAR-LC, Mr. E. Kelly
1	DRDAR-LCA, Dr. Sharkoff
1	DRDAR-LCE, Dr. Walker
2	DRDAR-QAS, Mr. F. Fitzsimmons
1	DRDAR-SCM, Mr. J. Corrie
1	DRDAR-TSP, Mr. B. Stephans
2	DRDAR-TSS, (STINFO)
	Commander, Aberdeen Proving Ground, Maryland 21005
3	ATTN: Technical Library, Building 313
	Commander, U. S. Army Foreign Science and Technology Center, 220 7th Street, N. E., Charlottesville, Virginia 22901
1	ATTN: DRXST-SD3
	Commander, Rock Island Arsenal, Rock Island, Illinois 61201
1	ATTN: SARRI-RDL
	Director, Eustis Directorate, U. S. Army Air Mobility Research & Development Laboratory, Fort Eustis, Virginia 23604
1	ATTN: SAVDL-EU-SS, Mr. J. Robinson
	Commander, U. S. Army Ballistic Research Laboratories, Aberdeen Proving Ground, Maryland 21005
1	ATTN: Dr. D. Eichelberger
	Director, U. S. Army Materiel Systems Analysis Activity, Aberdeen Proving Ground, Maryland 21005
1	ATTN: AMXSY-D, Dr. J. Sperrazza
	Commander, U. S. Army Mobility Equipment Research & Development Center, Fort Belvoir, Virginia 22060
2	ATTN: Technical Documents Center, Building 315
	Commander, U. S. Army Production Equipment Agency, Manufacturing Technology Branch, Rock Island Arsenal, Illinois 61202
1	ATTN: AMXPE, Mr. Ralph Siegel
	Commander, U. S. Army Research and Engineering Directorate, Warren, Michigan 48090
1	ATTN: SMOTA-RCM.1, Mr. Edward Moritz
1	SMOTA-RCM.1, Mr. Donald Phelps

No. of Copies	To
	Commander, Watervliet Arsenal, Watervliet, New York 12189
1	ATTN: SARWV-R
1	Dr. Robert Weigle
1	Chief, Bureau of Naval Weapons, Department of the Navy, Room 2225, Munitions Building, Washington, D. C.
	Chief, Bureau of Ships, Department of the Navy, Washington, D. C. 20315
1	ATTN: Code 341
	Chief of Naval Research, Arlington, Virginia 22217
1	ATTN: Code 472
	Headquarters, U. S. Air Force/RDPI, The Pentagon, Washington, D. C. 20330
1	ATTN: Major Donald Sponberg
	Headquarters, Aeronautical Systems Division, 4950 TEST W/TZHM (DH 2-5 Mgr), Wright-Patterson Air Force Base, Ohio 45433
1	ATTN: AFML-MATB, Mr. George Glenn
2	AFML-MXE, E. Morrissey
1	AFML-LLP, D. M. Forney, Jr.
1	AFML-LC
1	AFML-MBC, S. Schulman
	National Aeronautics and Space Administration, Washington, D. C. 20546
1	ATTN: AFSS-AD, Office of Scientific & Technical Information
1	Mr. B. G. Achhammer
1	Mr. G. C. Deutsch, Chief, Materials Research Program, Code RR-1
	National Aeronautics and Space Administration, Lewis Research Center, 21000 Brookpark Road, Cleveland, Ohio 44135
1	ATTN: Mr. G. Mervin Ault, Assistant Chief, M&S Division
	National Aeronautics and Space Administration, Marshall Space Flight Center, Huntsville, Alabama 35812
1	ATTN: S&E-ME-MM, Mr. W. A. Wilson, Building 4720
1	R-P&VE-M, R. J. Schwinghamer
	Albany Metallurgy Research Center, Albany, Oregon 97321
1	ATTN: Mr. R. R. Wells, Research Director
	Defense Materials Service, General Services Administration, Washington, D. C. 20405
1	ATTN: Mr. Clarence A. Fredell, Director, Technical R&D Staff
	Director, Army Materials and Mechanics Research Center, Watertown, Massachusetts 02172
2	ATTN: DRXMR-PL
1	DRXMR-PR
1	DRXMR-AP
1	DRXMR-CT
14	Author

Army Materials and Mechanics Research Center
Watertown, Massachusetts 02172
MAGNETIC PERTURBATION INSPECTION
OF ARTILLERY PROJECTILES
Russell D. Williams and John R. Barton,
Southwest Research Institute, 8500 Culebra
Road, P.O. Drawer 28510, San Antonio,
Texas 78284
Technical Report AMMRC CTR 77-23, September 1977, 66 pp -
illus - tables, Contract DAAG46-76-C-0075,
D/A Project N/A, AMCMS Code 4932.05.6654.0.02
Final Report, 8 Sept. 1976 through 7 Oct. 1977

AD________________

UNCLASSIFIED
UNLIMITED DISTRIBUTION

Key Words

Nondestructive Testing
Projectiles
Cylindrical Shells
Magnetic Detection
Defects

The objectives of this research were to determine feasibility for the application of magnetic perturbation inspection methods to interior and exterior surfaces of artillery projectile casings. Inspections were performed on ten (10) projectiles. Subsequent metallurgical sectioning at seven (7) magnetically determined sites confirmed flaws at all selected locations. Feasibility of method was demonstrated. Basic conceptual design of a prototype inspection device is included.

Army Materials and Mechanics Research Center
Watertown, Massachusetts 02172
MAGNETIC PERTURBATION INSPECTION
OF ARTILLERY PROJECTILES
Russell D. Williams and John R. Barton,
Southwest Research Institute, 8500 Culebra
Road, P.O. Drawer 28510, San Antonio,
Texas 78284
Technical Report AMMRC CTR 77-23, September 1977, 66 pp -
illus - tables, Contract DAAG46-76-C-0075,
D/A Project N/A, AMCMS Code 4932.05.6654.0.02
Final Report, 8 Sept. 1976 through 7 Oct. 1977

AD________________

UNCLASSIFIED
UNLIMITED DISTRIBUTION

Key Words

Nondestructive Testing
Projectiles
Cylindrical Shells
Magnetic Detection
Defects

The objectives of this research were to determine feasibility for the application of magnetic perturbation inspection methods to interior and exterior surfaces of artillery projectile casings. Inspections were performed on ten (10) projectiles. Subsequent metallurgical sectioning at seven (7) magnetically determined sites confirmed flaws at all selected locations. Feasibility of method was demonstrated. Basic conceptual design of a prototype inspection device is included.

Army Materials and Mechanics Research Center
Watertown, Massachusetts 02172
MAGNETIC PERTURBATION INSPECTION
OF ARTILLERY PROJECTILES
Russell D. Williams and John R. Barton,
Southwest Research Institute, 8500 Culebra
Road, P.O. Drawer 28510, San Antonio,
Texas 78284
Technical Report AMMRC CTR 77-23, September 1977, 66 pp -
illus - tables, Contract DAAG46-76-C-0075,
D/A Project N/A, AMCMS Code 4932.05.6654.0.02
Final Report, 8 Sept. 1976 through 7 Oct. 1977

AD________________

UNCLASSIFIED
UNLIMITED DISTRIBUTION

Key Words

Nondestructive Testing
Projectiles
Cylindrical Shells
Magnetic Detection
Defects

The objectives of this research were to determine feasibility for the application of magnetic perturbation inspection methods to interior and exterior surfaces of artillery projectile casings. Inspections were performed on ten (10) projectiles. Subsequent metallurgical sectioning at seven (7) magnetically determined sites confirmed flaws at all selected locations. Feasibility of method was demonstrated. Basic conceptual design of a prototype inspection device is included.

Army Materials and Mechanics Research Center
Watertown, Massachusetts 02172
MAGNETIC PERTURBATION INSPECTION
OF ARTILLERY PROJECTILES
Russell D. Williams and John R. Barton,
Southwest Research Institute, 8500 Culebra
Road, P.O. Drawer 28510, San Antonio,
Texas 78284
Technical Report AMMRC CTR 77-23, September 1977, 66 pp -
illus - tables, Contract DAAG46-76-C-0075,
D/A Project N/A, AMCMS Code 4932.05.6654.0.02
Final Report, 8 Sept. 1976 through 7 Oct. 1977

AD________________

UNCLASSIFIED
UNLIMITED DISTRIBUTION

Key Words

Nondestructive Testing
Projectiles
Cylindrical Shells
Magnetic Detection
Defects

The objectives of this research were to determine feasibility for the application of magnetic perturbation inspection methods to interior and exterior surfaces of artillery projectile casings. Inspections were performed on ten (10) projectiles. Subsequent metallurgical sectioning at seven (7) magnetically determined sites confirmed flaws at all selected locations. Feasibility of method was demonstrated. Basic conceptual design of a prototype inspection device is included.